NMR and EPR Studies of Low-Spin Fe(III) Complexes of m eso -Tetra-(2,6-Disubstituted Phenyl)Porphyrinates Complexed to Imidazoles and Pyridines of Widely Differing Basicities

ARTICLE *in* INORGANIC CHEMISTRY · OCTOBER 2005

Impact Factor: 4.76 · DOI: 10.1021/ic0507316 · Source: PubMed

4 AUTHORS, INCLUDING:

F(rances) Ann Walker
The University of Arizona
242 PUBLICATIONS **9,001** CITATIONS

SEE PROFILE

Inorg. Chem. **2005**, *44*, 7468–7484

NMR and EPR Studies of Low-Spin Fe(III) Complexes of *meso*-Tetra-(2,6-Disubstituted Phenyl)Porphyrinates Complexed to Imidazoles and Pyridines of Widely Differing Basicities

C. Todd Watson,[†] Sheng Cai,[‡] Nikolai V. Shokhirev, and F. Ann Walker*

Department of Chemistry, University of Arizona, Tucson, Arizona 85721-0041

Received May 10, 2005

A series of bis-axially ligated complexes of iron(III) tetramesitylporphyrin, TMPFe(III), tetra-(2,6-dibromophenyl)-porphyrin, $(2,6\text{-Br}_2)_4$TPPFe(III), tetra-(2,6-dichlorophenyl)porphyrin, $(2,6\text{-Cl}_2)_4$TPPFe(III), tetra-(2,6-difluorophenyl)-porphyrin, $(2,6\text{-F}_2)_4$TPPFe(III), and tetra-(2,6-dimethoxyphenyl)porphyrin, $(2,6\text{-(OMe)}_2)_4$TPPFe(III), where the axial ligands are 1-methylimidazole, 2-methylimidazole, and a series of nine substituted pyridines ranging in basicity from 4-(dimethylamino)pyridine ($pK_a(PyH^+) = 9.70$) to 3- and 4-cyanopyridine ($pK_a(PyH^+) = 1.45$ and 1.1, respectively), have been prepared and characterized by EPR and ^{1}H NMR spectroscopy. The EPR spectra, recorded at 4.2 K, show "large g_{max}", rhombic, or axial signals, depending on the iron porphyrinate and axial ligand, with the g_{max} value decreasing as the basicity of the pyridine decreases, thus indicating a change in electron configuration from $(d_{xy})^2(d_{xz},d_{yz})^3$ to $(d_{xz},d_{yz})^4(d_{xy})^1$ through each series at this low temperature. Over the temperature range of the NMR investigations (183–313 K), most of the high-basicity pyridine complexes of all five iron(III) porphyrinates exhibit simple Curie temperature dependence of their pyrrole-H paramagnetic shifts and β-pyrrole spin densities, $\rho_C \approx 0.015$–0.017, that are indicative of the $S = 1/2$ $(d_{xy})^2(d_{xz},d_{yz})^3$ electron configuration, while the temperature dependences of the pyrrole-H resonances of the lower-basicity pyridine complexes ($pK_a(PyH^+) < 6.00$) show significant deviations from simple Curie behavior which could be fit to an expanded version of the Curie law using a temperature-dependent fitting program developed in this laboratory that includes consideration of a thermally accessible excited state. In most cases, the ground state of the lower-basicity pyridine complexes is an $S = 1/2$ state with a mixed $(d_{xy})^2(d_{xz},d_{yz})^3/(d_{xz},d_{yz})^4(d_{xy})^1$ electron configuration, indicating that these two are so close in energy that they cannot be separated by analysis of the NMR shifts; however, for the TMPFe(III) complexes with 3- and 4-CNPy, the ground states were found to be fairly pure $(d_{xz},d_{yz})^4(d_{xy})^1$ electron configurations. In all but one case of the intermediate- to low-basicity pyridine complexes of the five iron(III) porphyrinates, the excited state is found to be $S = 3/2$, with a $(d_{xz},d_{yz})^3(d_{xy})^1(d_{z^2})^1$ electron configuration, lying some 120–680 cm^{-1} higher in energy, depending on the particular porphyrinate and axial ligand. Full analysis of the paramagnetic shifts to allow separation of the contact and pseudocontact contributions could be achieved only for the $[TMPFe(L)_2]^+$ series of complexes.

Introduction

Synthetic ferriheme complexes of various types have been shown to be very promising models of the heme centers in the mitochondrial cytochrome bc_1 complex and other related heme proteins.[1−11] For this reason, a detailed investigation of their NMR and frozen solution EPR spectra is highly desirable. While EPR spectroscopy is an excellent technique

* To whom correspondence should be addressed. Phone: 520-621-8645. Fax: 520-626-9300. E-mail: awalker@u.arizona.edu.

[†] Current address: Department of Chemistry, MS324, Unversity of Arkansas, 5210 Grand Ave., Fort Smith, AR 72913-3649. E-mail: cwatson@uafortsmith.edu.

[‡] Current address: Division of Immunology, City of Hope National Medical Center, 1500 E Duarte Rd., Duarte, CA 91010. E-mail: SCai@coh.org.

(1) Walker, F. A.; Huynh, B. H.; Scheidt, W. R.; Osvath, S. R. *J. Am. Chem. Soc.* **1986**, *108*, 5288−5297.
(2) Walker, F. A.; Benson, M. *J. Phys. Chem. Soc.* **1982**, 88, 3495−3499.
(3) Safo, M. K.; Gupta, G. P.; Walker, F. A.; Scheidt, W. R. *J. Am. Chem. Soc.* **1991**, *113*, 5497−5510.
(4) Safo, M. K.; Gupta, G. P.; Watson, C. T.; Simonis, U.; Walker, F. A.; Scheidt, W. R. *J. Am. Chem. Soc.* **1992**, *114*, 7066−7075.
(5) Safo, M. K.; Walker, F. A.; Raitsimring, A. M.; Walters, W. P.; Dolata, D. P.; Debrunner, P. G.; Scheidt, W. R. *J. Am. Chem. Soc.* **1994**, *116*, 7760−7770.

10.1021/ic0507316 CCC: $30.25
Published on Web 09/03/2005

for characterizing the electronic ground state of ferriheme complexes at 4.2 K, as we have shown in studies of the molecular structures and EPR spectra of a number of porphyrinate complexes of Fe(III) in the solid state,[1,3−5,9,11] NMR spectroscopy is extremely useful for investigating the ambient-temperature solution structures and spin states of a wide range of metalloporphyrins.[6−8,12−15] As part of an ambient-temperature study, it is often possible not only to characterize the electronic ground state but also to determine the possible existence of a thermally accessible excited state, as we have shown elsewhere.[8,12−15] This is because of the temperature dependence of the paramagnetic contribution to the chemical shift of a given proton, also known as the hyperfine or isotropic shift, as shown below.

The chemical shifts of protons in the NMR spectra of paramagnetic molecules are the sum of two contributions, the first of which is the diamagnetic shift, the chemical shift of the protons of interest in the absence of unpaired electrons in the molecule. An accurate approximation of the diamagnetic shift can be obtained from a diamagnetic compound that is similar to the paramagnetic one being studied,[6] herein the Co(III) analogues of the Fe(III) complexes of this study. The second contribution to the observed chemical shift is the paramagnetic shift, which is also known as the isotropic or hyperfine shift[6,16−19]

$$\delta_{obs} = \delta_{dia} + \delta_{para} \quad (1)$$

$$\delta_{para} = \delta_{iso} = \delta_{hf} \quad (2)$$

The paramagnetic shift can be subdivided into two parts, the contact and electron−nuclear dipolar (pseudocontact) contributions[6,16−19]

$$\delta_{para} = \delta_{con} + \delta_{pc} \quad (3)$$

The contact term represents the paramagnetic shift of the resonance from the diamagnetic position caused by the delocalization of the unpaired electron through bonds[6,16−19]

$$\delta_{con} = A\langle g\rangle\beta S(S+1)\mu_0/12\pi\gamma_N h k_B T \quad (4)$$

In this equation, A is the electron−nuclear hyperfine coupling constant, $\langle g\rangle$ is the average g value, S is the total spin of the metal (which is 1/2 for the systems of interest in this work), β is the Bohr magneton (9.2741×10^{-28} J G^{-1}), h is Planck's constant divided by 2π (1.6784×10^{-35} J s), k_B is the Boltzmann constant (1.3806×10^{-23} J K^{-1}), μ_0 is the permittivity of a vacuum, and γ_N is the magnetogyric ratio of the NMR nucleus. If the delocalization occurs through σ bonds the sign of the contact shift is positive.[20] This results in a positive shift of the resonance.[6,16] If the delocalization occurs through π bonds, the sign of the contact shift for a proton attached to a carbon that is part of the π system is negative[6,16−22] and the observed shift is negative.[6,16−19]

The other contribution to the paramagnetic shift of eq 3 is the pseudocontact shift. This results from the through-space interaction between the unpaired electron at the metal center and the nucleus being studied and may be approximated as the following if the second-order Zeeman contribution to the magnetic susceptibilities is small and the ground state is well-separated from any excited states[6,23]

$$\delta_{pc} = [\beta^2 S(S+1)\mu_0/72\pi k_B T]\{[2g_{zz}^2 - (g_{xx}^2 + g_{yy}^2)](3\cos^2\theta - 1)/r^3 + 3(g_{xx}^2 - g_{yy}^2)(\sin^2\theta\cos 2\Omega)/r^3\} \quad (5)$$

For systems with axial symmetry or 4-fold-symmetric macrocyclic complexes with rapidly rotating axial ligands, the last term of eq 5, the rhombic part, averages to zero, leaving[6,16−19]

$$\delta_{pc} = [\beta^2 S(S+1)\mu_0/72\pi k_B T][2g_{zz}^2 - (g_{xx}^2 + g_{yy}^2)](3\cos^2\theta - 1)/r^3 \quad (6)$$

In eqs 5 and 6, g_{zz}, g_{yy}, and g_{xx} are the principal g values of the metal complex, where g_{zz} is the g value along the molecular z axis, which is aligned with the heme normal, r is the distance from the metal center to the proton of interest, and θ is the angle between a line along the magnetic z axis, usually taken to be the molecular z axis, and a line running through the metal center and the position of interest. Goff has shown[24] that for bis-imidazole complexes of iron(III) porphyrinates the quantity $[2g_{zz}^2 - (g_{xx}^2 + g_{yy}^2)]$ is very similar whether calculated from EPR g values or from NMR data, suggesting that the second-order Zeeman term[23] is probably quite small for these bis-imidazole complexes. However, we found, in the work discussed below, that the

(6) Walker, F. A. Proton NMR and EPR Spectroscopy of Paramagnetic Metalloporphyrins. In *The Porphyrin Handbook*; Kadish, K. M., Smith, K. M., Guilard, R., Eds.; Academic Press: San Diego, CA, 2000; Vol. 5, Chapter 36, pp 81−183.
(7) La Mar, G. N.; Bold, T. J.; Satterlee, J. D. *Biochim. Biophys. Acta* **1977**, *498*, 189−207.
(8) Basu, P.; Shokhirev, N. V.; Enemark, J. H.; Walker, F. A. *J. Am. Chem. Soc.* **1995**, *117*, 9042−9055.
(9) Yatsunyk, L. A.; Carducci, M. D.; Walker, F. A. *J. Am. Chem. Soc.* **2003**, *125*, 15986−16005.
(10) Walker, F. A. *Coord. Chem. Rev.* **1999**, *185−186*, 471−534.
(11) Walker, F. A. *Chem. Rev.* **2004**, *104*, 589−615.
(12) Shokhirev, N. V.; Walker, F. A. *J. Phys. Chem.* **1995**, *99*, 17795−17804.
(13) Nesset, M. J. M.; Cai, S.; Shokhireva, T. Kh.; Shokhirev, N. V.; Jacobson, S. E.; Jayaraj, K.; Gold, A.; Walker, F. A. *Inorg. Chem.* **2000**, *39*, 532−540.
(14) Banci, L.; Bertini, I.; Luchinat, C.; Pierattelli, R.; Shokhirev, N. V.; Walker, F. A. *J. Am. Chem. Soc.* **1998**, *120*, 8472−8479.
(15) Yatsunyk, L. A.; Shokhirev, N. V.; Walker, F. A. *Inorg. Chem.* **2005**, *44*, 2848−2866.
(16) La Mar, G. N.; Walker, F. A. NMR Studies of Paramagnetic Metalloporphyrins. In *The Porphyrins*, Vol. IV; Dolphin, D., Ed.; Academic Press: New York, 1979; pp 61−157.
(17) Bertini, I.; Luchinat, C.; Parigi, G. *Solution NMR of Paramagnetic Molecules. Applications to Metallobiomolecules and Models*; Elsevier: New York, 2001.
(18) Walker, F. A. *Inorg. Chem.* **2003**, *42*, 4526−4544.
(19) Kurland, R. J.; McGarvey, B. R. *J. Magn. Reson.* **1970**, *2*, 286−301.
(20) Carrington, A.; McLachlan, A. D. *Introduction to Magnetic Resonance*; Harper and Row: New York, 1967; p 80.
(21) McLachlan, A. D. *Mol. Phys.* **1958**, *1*, 233.
(22) Chestnut, D. B. *J. Chem. Phys.* **1958**, *29*, 43−47.
(23) Horrocks, W. D.; Greenberg, E. S. *Mol. Phys.* **1974**, *27*, 993−999.
(24) Goff, H. M. Nuclear Magnetic Resonance of Iron Porphyrins. In *Iron Porphyrins, Part One*; Lever, A. B. P., Gray, H. B., Eds; Addison-Wesley: Reading, MA, 1983; p 249.

EPR g values appear to overestimate the magnitude of the ambient temperature pseudocontact shifts of the bis-pyridine complexes of the iron porphyrinates of this study.

As is evident from eqs 4−6, both the contact and pseudocontact shifts usually have inverse temperature dependences resulting from the Curie law[6,16−19,25]

$$\delta_{\text{para}} = C/T \tag{7}$$

where C is the Curie coefficient.

Because the contact term dominates the paramagnetic shifts of all spin states of Fe(III), a nearly linear $1/T$ dependence is generally observed even for the $S = 5/2$ Fe(III) complexes,[19] which have the largest zero-field splitting constants for this metal and oxidation state.[16] However, as we have shown previously,[12−15,26−28] a number of model heme complexes have a thermally-accessible excited state that causes at least some curvature of the Curie plot[8,12,14,15,27,28] and can sometimes show extremely curved chemical-shift dependence.[13,15,26] Expansion of the Curie law to include the contribution from the Boltzmann population of this thermally-accessible excited state yields the following expression, if the $1/T^2$ contribution to the high-spin state is neglected[12−16,19]

$$\delta_{\text{para}} = (1/T)[W_1C_{n1} + W_2C_{n2}\, e^{-\Delta E/kT}]/[W_1 + W_2\, e^{-\Delta E/kT}] \tag{8}$$

In this equation, C_{n1} is the coefficient for the position of interest for level 1, C_{n2} is the coefficient for the position of interest for level 2, W_1 and W_2 are the statistical weights for each level ($= 2S + 1$ for each), and ΔE is the energy separation between the two levels. The coefficients C_{n1} and C_{n2} are approximately equal to the Curie coefficients of each level, except for the contribution from the pseudocontact contribution to δ_{para}, and can be determined by fitting the temperature dependence of the proton chemical shifts, assuming that the diamagnetic shift of each proton type is known. Each of these coefficients can be further decomposed into the McConnell constant Q_C and the variable ρ_C, where $Q_C = -496.8$ ppm K for aromatic carbons,[16,20−22] and ρ_C is the spin density at the carbon of interest; in general ρ_C is not larger than about 0.02 for the systems of this study. A program that carries out this fitting procedure, with least-squares minimization of the errors between the experimental and calculated shifts, has been created in our laboratory and is available on the Internet.[29]

The bis-ligand (imidazoles and pyridines of widely differing basicities) complexes of several iron(III) octaalkyltetraphenylporphyrinates have been prepared and characterized by X-ray crystallography,[9,26−28] EPR,[9,14,26−28] NMR,[15,26−28] and in some cases, Mössbauer spectroscopy.[30] The NMR investigations of these complexes showed that although the ground state differs for various axial ligand complexes and is usually fully consistent with that observed by EPR spectroscopy at 4.2 K, the excited state often has $S = 3/2$ (or $S = 5/2$ in the cases where the ground state has $S = 3/2$).[15,26,27]

Scheme 1

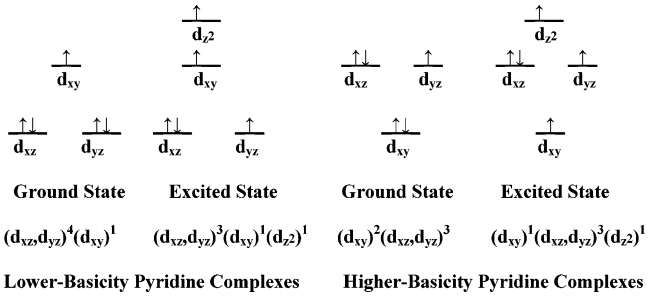

Earlier, many of the same bis-ligand complexes of iron(III) tetramesitylporphyrinate were prepared and characterized by X-ray crystallography, EPR, Mössbauer,[3,4,31] and to a limited extent, NMR[4] spectroscopy, although no detailed analysis of the temperature dependence of the NMR spectra was made at that time. To further examine the effects of the axial ligand basicity and the 2,6-phenyl substituents on the orientation of planar axial ligands and NMR properties of these supposedly "hindered" porphyrin systems, an investigation of the variable-temperature ^{1}H NMR spectra of TMPFe(III) and a series of 2,6-disubstituted tetraphenylporphyrinatoiron(III) with axial ligands were undertaken in this work. The Mössbauer spectra of several $[((2,6\text{-}OCH_3)_2)_4\text{-}TPPFe(L)_2]^+$, $[TPPFe(L)_2]^+$, and $[TPCFe(L)_2]^+$ complexes that show differences in quadrupole splittings and hyperfine coupling constants as a function of axial imidazole and pyridine ligands have also been reported.[32] All complexes are low-spin d^5, $S = 1/2$. However, as shown previously for several $[TMPFe(L)_2]^+$ complexes,[4] there are two electron configurations possible for low-spin Fe(III), the $(d_{xy})^2(d_{xz},d_{yz})^3$ and $(d_{xz},d_{yz})^4(d_{xy})^1$ configurations, as shown in Scheme 1. The electron configuration of a given complex was found to depend on the nature of the porphyrin substituents and, within a given set of porphyrin substituents, upon the σ-donor and π-donor/acceptor properties of the axial ligands. The σ-donor strengths, within a series of closely related ligands such as substituted pyridines of varying basicities toward the proton, are usually measured by the pK_a values of the conjugate acid of the particular pyridine, here abbreviated as pK_a(PyH$^+$), or by the gas-phase lone-pair vertical ionization potentials of the substituted pyridines, which are in general linearly related to the pK_a(PyH$^+$) values.[33]

As shown previously for several bis-pyridine complexes of TMPFe(III), as the basicity of the pyridine decreases from

(25) This is true except in the cases where $S > 1/2$ and there is a relatively large zero-field splitting, in which case the pseudocontact term has a C'/T^2 dependence and the contact term has a C/T dependence.[6,16−19]
(26) Yatsunyk, L. A.; Walker, F. A. *Inorg. Chem.* **2004**, *43*, 757−777.
(27) Yatsunyk, L. A.; Walker, F. A. *Inorg. Chem.* **2004**, *43*, 4341−4352.
(28) Yatsunyk, L. A.; Walker, F. A. *J. Porphyrins Phthalocyanines* **2005**, *9*, 214−228.
(29) Shokhirev, N. V.; Walker, F. A. http://www.shokhirev.com/nikolai/programs/prgsciedu.html.
(30) Teschner, T.; Yatsunyk, L. A.; Schünemann, V.; Hu, C.; Scheidt, W. R.; Walker, F. A.; Trautwein, A. X. *J. Am. Chem. Soc.* , Submitted for publication, 2005.
(31) Munro, O. Q.; Marques, H. M.; Debrunner, P. G.; Mohanrao, K.; Scheidt, W. R. *J. Am. Chem. Soc.* **1995**, *117*, 935−954.
(32) Benda, R.; Schünemann, V.; Trautwein, A. X.; Cai, S.; Polam, J. R.; Watson, C. T.; Shokhireva, T. Kh.; Walker, F. A. *J. Biol. Inorg. Chem.* **2003**, *8*, 787−801.
(33) Ramsey, B. G.; Walker, F. A. *J. Am. Chem. Soc.* **1974**, *96*, 3314−3316.

that of 4-Me_2NPy ($pK_a(PyH^+) = 9.70$[34]) to that of 4-CNPy ($pK_a(BH^+) \approx 1.1$[4]), the electronic ground state of the complex appears to shift fairly smoothly from $(d_{xy})^2(d_{xz},d_{yz})^3$ to $(d_{xz},d_{yz})^4(d_{xy})^1$, as evidenced by trends in the size of the largest EPR *g* value,[3−5] the Mössbauer quadrupole splitting,[3,4] or the NMR pyrrole-H chemical shift.[4] At the time of the earlier report,[4] we believed that there were only those two $S = 1/2$ electron configurations involved, with a variable ΔE between the two. However, the present work has shown conclusively that the energy separation between these two is, in most cases, extremely small, so that a mixed-configuration $S = 1/2$ ground state is present for many of the complexes of this study, and instead, the excited state has $S = 3/2$. Two limiting types of EPR spectra, each of which usually consists of only one resolved feature, were observed in this study; if the single observed feature had its maximum at $g > 3.2$, it was called a "large g_{max}" EPR spectrum[4] because the largest *g* value of the normal rhombic EPR spectra of the low-spin Fe(III) porphyrinates, in which all three *g* values are readily observed, typically are not significantly greater than 3.0. If this feature occurred at $g \leq 2.6$, it was shown to be the $g_\perp$ of an axial EPR spectrum, and in some cases, the corresponding $g_{||}$ feature was also resolved and observed at $g < 2.0$.[4] However, it was not known at the time of that study that the energy separation of the two electron configurations was so small that intermediate- to low-basicity pyridines behave as though they have a mixed-configuration low-spin state over the temperature range of the NMR investigations (183−313 K), and no energy separation between the two can be determined, even though the EPR spectra measured at 4.2 K clearly show a smooth trend.[4] In the present study, we have carefully analyzed the temperature dependence of the ^{1}H NMR spectra of the $[TMPFe(L)_2]^+$ complexes, where L = a series of nine pyridines of varying basicities, as well as two imidazoles, and have extended our investigation of the ^{1}H NMR and EPR spectra to include the corresponding complexes of the following phenyl-substituted iron porphyrinates, $[(2,6\text{-}Br_2)_4TPPFe\text{-}(L)_2]^+$, $[(2,6\text{-}Cl_2)_4TPPFe(L)_2]^+$, $[(2,6\text{-}F_2)_4\text{-}TPPFe(L)_2]^+$, and $[(2,6\text{-}(OMe)_2)_4TPPFe(L)_2]^+$, in an attempt to understand the composition of the paramagnetic shifts of the porphyrin and axial ligand protons and the nature of the excited states of these complexes. For the octaalkyltetraphenylporphyrinates,[15,26,27] most of the intermediate- and low-basicity pyridine complexes of the present study have $S = 3/2$ excited states.

Experimental

$TMPH_2$ and $(2,6\text{-}Cl_2)_4TPPH_2$ were purchased from Mid Century or prepared as described previously;[13,35] the $(2,6\text{-}X_2)_4TPPH_2$ free-base porphyrins were synthesized as described previously.[13,35] TMPFeCl, $(2,6\text{-}Br_2)_4TPPFeCl$, $(2,6\text{-}Cl_2)_4TPPFeCl$, $(2,6\text{-}F_2)_4TPPFeCl$, and $2,6\text{-}(OMe)_2)_4TPPFeCl$ and their perchlorate complexes were synthesized from the corresponding free-base porphyrins as described previously.[13,35] The bis-pyridine and bis-imidazole complexes were produced as follows: Roughly 5 mg of the desired iron(III) porphyrin perchlorate and 0.35 mL of CD_2Cl_2 were added to a 5 mm NMR tube. Several milligrams of the desired axial ligand were added to this solution. The ^{1}H NMR spectrum was then recorded. At this point, more ligand was titrated into the NMR tube until the 1D NMR spectra showed free ligand resonances at −60 °C. The iron porphyrinate concentrations were 10 to 15 mM. The dilution of these concentrations by factors of 2 to 4 caused no changes in the chemical shifts of the protons of the bis-imidazole or -pyridine complexes. All ligands were used as received from Aldrich. The 99.9% CD_2Cl_2 was used as received in 1 g sealed ampules from Cambridge Isotopes.

The ^{1}H NMR spectra of $[TMPFe(L)_2]ClO_4$, $[(2,6\text{-}Br_2)_4TPPFe\text{-}(L)_2]ClO_4$, $[(2,6\text{-}Cl_2)_4TPPFe(L)_2]ClO_4$, $[2,6\text{-}F_2TPPFe(L)_2]ClO_4$, and $[(2,6\text{-}(OMe)_2)_4TPPFe(L)_2]ClO_4$, where L = axial ligands 4-CNPy, 3-CNPy, 3-ClPy, 4-HPy, 3-MePy, 4-MePy, 3,5-Me_2Py, 3,4-Me_2Py, 4-Me_2NPy, 1-MeIm, and 2-MeHIm, were recorded on either a General Electric GN-300 spectrometer operating at 300.100 MHz, a Bruker AM-250 spectrometer operating at 250.068 MHz, a General Electric GN-500 spectrometer operating at 500.136 MHz, or a Varian Unity-300 spectrometer operating at 299.952 MHz. The number of data points was always 16 K, and the spectral width ranged from 7.5 to 40 kHz as necessary for the particular complex and spectrometer. The acquisition times ranged from 0.266 to 0.682 s, depending upon the relaxation times of the resonances being studied. The number of transients collected ranged from 128 to 256, and a 5 Hz line broadening factor to the exponential multiplication of the FID was usually applied prior to the Fourier transformation. The spectra of the iron(III) porpyrinates were recorded at temperatures from −90 to +40 °C in 5 or 10° steps; the temperature was determined by calibration with the Wilmad standard methanol variable-temperature sample.

The EPR spectra of the iron(III) porphyrinates listed above were recorded at 4.2 K on a Bruker ESP-300E EPR spectrometer (operating at 9.4 GHz) equipped with an Oxford Instruments ESR 900 continuous flow helium cryostat. Microwave frequencies were measured using a Systron-Donner frequency counter. The spectra were obtained for samples in frozen CD_2Cl_2 and, in some cases, toluene solutions. Typical values for microwave power, modulation frequency, and modulation amplitude were 0.2 mW, 100 kHz and 1.011 G, respectively. The *g* values obtained from these spectra are listed in Table 1.

The synthesis of the bis-substituted pyridine and imidazole complexes of $(2,6\text{-}Br_2)_4TPPCo(III)$, $(2,6\text{-}Cl_2)_4TPPCo(III)$, $(2,6\text{-}F_2)_4\text{-}TPPCo(III)$, and $(2,6\text{-}(OMe)_2)_4TPPCo(III)$ were carried out as described elsewhere.[36] The 1D ^{1}H NMR spectra of these diamagnetic compounds were recorded on a Varian Unity-300 spectrometer operating at 299.952 MHz. The number of data points was again 16 K, and the spectral width ranged from 3.5 to 4.6 kHz. The acquisition times ranged from 1.737 to 2.318 s. The number of transients collected ranged from 128 to 256, and no exponential multiplication of the FID was applied prior to the Fourier transformation. The corresponding TMPCo(III) complexes were synthesized, and their ^{1}H NMR spectra were reported elsewhere.[43]

(34) Albert, A. In *Physical Methods in Heterocyclic Chemistry*; Katritzky, A. R., Ed.; Academic Press: New York, 1971; Vol. I, pp 1−108.
(35) Watson, C. T. The Effect of Axial Ligands and Porphyrin Substituents on the Electronic Ground State of Low-Spin Fe(III) Porphyrinates. Ph.D. Dissertation, University of Arizona, Tuscon, AZ, 1996.
(36) Polam, J. R.; Shokhireva, T. Kh.; Raffii, K.; Simonis, U.; Walker, F. A. *Inorg. Chim. Acta* **1997**, *263/1−2*, 109−117.
(37) Raitsimring, A. M.; Borbat, P.; Shokhireva, T. Kh.; Walker, F. A. *J. Phys. Chem.* **1996**, *100*, 5235−5244.
(38) Raitsimring, A. M.; Walker, F. A. *J. Am. Chem. Soc.* **1998**, *120*, 991−1002.
(39) Schünemann, V.; Raitsimring, A. M.; Benda, R.; Trautwein, A. X.; Shokhireva, T. Kh.; Walker, F. A. *J. Biol. Inorg. Chem.* **1999**, *4*, 708−716.

Table 1. EPR *g* Values of the Iron(III) Porphyrinates of This Study

		porphyrinate				
ligand	pK_a(BH^+)	TMP	(2,6-Br_2)$_4$TPP	(2,6-Cl_2)$_4$TPP	(2,6-F_2)$_4$TPP	(2,6-($OMe)_2$)$_4$TPP
4-Me_2NPy	9.70	3.48[a]	3.59	3.49	(2.70)2.60	2.83
					2.29	2.30
					1.86	(1.64) 1.62
4-NH_2Py	9.17	3.40[b]				
4-MePy	6.02	2.70[c]	3.19	3.25	3.48	3.43
		2.49[c]				1.90
3-EtPy	5.56	2.89[b]				
4-HPy	5.22	2.75[c]	2.99	2.90[b]	3.41	2.52
		2.56[c]		2.20[b]		
3-ClPy	2.84	3.07[b,c]	3.01[b]	2.63		2.60
		2.59[c]	2.57[b]			
3-CNPy	1.45	2.64[b]	2.62	2.62		2.60
4-CNPy	1.1	2.53[b]	2.57	2.51	2.57	2.58
		1.54[b]				
2-MeHIm	7.56	3.17	3.43	3.42	3.52	3.35
1-MeIm	7.33	2.89[a]	3.36	2.88	2.84	3.02
		2.33[a]		2.30	2.29	2.28
		1.57[a]		1.60	1.63	1.48
		(1.49)[d]	(1.55)[d]	(1.64)[d]	(1.30)[d]	

[a] Ref 3. [b] Ref 4. [c] The two numbers given indicate the range of *g* values encompassed by the very broad signal. [d] The number in parentheses is the smallest *g* value, calculated from $\sum g^2 = 16.0$.

Ambient-temperature ^{1}H NMR chemical shifts of the free-base, chloroiron(III), and perchloratoiron(III) complexes of the five porphyrinates under study are listed in Supporting Information Tables S1, S2, and S3, respectively.

Results

EPR Spectra of the (2,6-X_2)$_4$TPPFe(III) Bis-pyridine and Bis-imidazole Complexes. In Figure 1 are shows examples of the general EPR spectral types of rhombic (also called Type II[10]), axial (also called Type III[10]), and large g_{max} (also called Type I[10]) porphyrinatoiron(III) bis-ligand complexes. As has been shown elsewhere,[9−11] both rhombic and "large g_{max}" EPR spectra are observed for low-spin ferriheme systems with $(d_{xy})^2(d_{xz},d_{yz})^3$ electron configurations and planar axial ligands in parallel and perpendicular planes, respectively, while axial EPR spectra are observed for low-spin ferriheme systems with $(d_{xz},d_{yz})^4(d_{xy})^1$ electron configurations. Most of the complexes of this study (except for those of 1-MeIm for all but one of the porphyrinates) have axial ligands in perpendicular planes and thus give "large g_{max}" or Type I[10] EPR spectra for the high-basicity pyridine complexes and axial or Type III[10] EPR spectra for the lowest-basicity pyridine complexes; the complexes of intermediate-basicity pyridines typically gave broad signals (Figure 1e, for example) that were difficult to characterize in terms of the electron configuration of the metal, and because of the short relaxation times, it has not been possible to determine unambiguously the electron configuration of these by pulsed EPR spectroscopy as we have done in other cases of questionable ground-state complexes.[37−41] The *g* values obtained for the complexes are listed in Table 1. Those of some of the TMP complexes have been reported and discussed previously,[3,4] and it was shown that the g_{max} values (as well as the Mössbauer quadrupole splittings) decrease as the basicity of the axial pyridine ligand decreases. However, some of the EPR spectra are extremely broad (like the one shown in Figure 1e), and in these cases, we report a range of *g* values, as listed in Table 1. As is evident from the *g* values of Table 1, the other porphyrinates of this study show similar ranges of *g* values for the various axial ligands, except the 4-Me_2NPy complexes of (2,6-F_2)$_4$TPPFe(III) and (2,6-(OMe_2))$_4$TPPFe(III) which have rhombic EPR signals, presumably because the ortho substituents in these two cases are small enough to allow the ligands to bind in near-parallel planes; along the same lines, the 1-MeIm complex of (2,6-Br_2)$_4$TPPFe(III) is the only one of the 1-MeIm complexes to exhibit a single-feature large g_{max} EPR signal, presumably because of the large size of the *ortho*-bromo substituents, which must encourage the porphyrinate ring to ruffle and thus cause even the five-membered ring 1-MeIm ligands to bind in perpendicular planes.

It has been assumed for some time that g_{max} values of greater than 3.2 are indicative of the $(d_{xy})^2(d_{xz},d_{yz})^3$ electron configuration,[1] for which this g_{max} is aligned along the normal to the heme plane, while for g_{max} values of 2.6 or less the electron configuration is $(d_{xz},d_{yz})^4(d_{xy})^1$ and this g_{max} is oriented in the *xy* plane and is thus g_x,g_y or $g_\perp$, with g_z being the smallest *g* value.[4,6,10,37−41] These assumptions were strongly supported by low-temperature near-infrared MCD spectra of [TMPFe(1-MeIm)$_2$]$^+$, [TMPFe(4-Me_2NPy)$_2$]$^+$, and [TMPFe(4-CNPy)$_2$]$^+$,[42] for which the first two complexes showed fairly intense near-IR bands near 1160 and 1400 nm at 4.2 K, while the third had extremely weak bands in the same wavelength region. This difference was explained by the fact that the porphyrin → Fe(III) charge-transfer transitions that give rise to the NIR bands are allowed when the hole is in the d_{xz},d_{yz} orbital set but are forbidden when it is in the d_{xy} orbital.[42] They are also strongly supported by the

(40) Astashkin, A. V.; Raitsimring, A. M.; Walker, F. A. *J. Am. Chem. Soc.* **2001**, *123*, 1905−1913.
(41) Astashkin, A. V.; Raitsimring, A. M.; Kennedy, A. R.; Shokhireva, T. Kh.; Walker, F. A. *J. Phys. Chem. A* **2002**, *106*, 74−82.
(42) Cheesman, M. R.; Walker, F. A. *J. Am. Chem. Soc.* **1996**, *118*, 8, 7373−7380.
(43) Rafii, K. NMR Studies of a Series of Porphyrinato Cobalt(II) and Cobalt(III) Complexes. M.S. Thesis, San Francisco State University, San Francisco, CA, 1993.

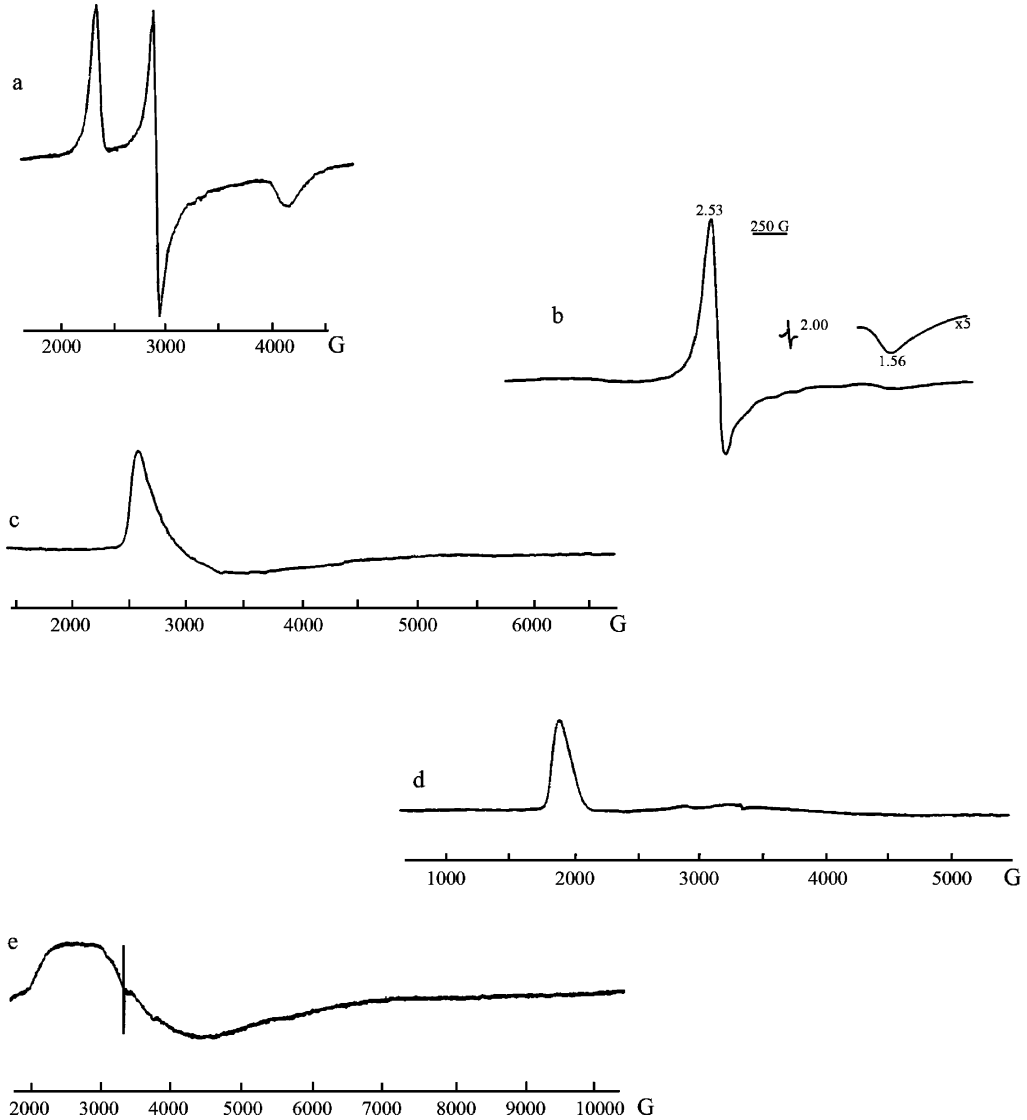

Figure 1. Examples of frozen solution EPR spectra observed for the low-spin Fe(III) porphyrinate complexes of this study: (a) rhombic, $[(2,6\text{-}F_2)_4TPPFe(1\text{-}MeIm)_2]ClO_4$; (b) axial with g_z resolved, $[TMPFe(4\text{-}CNPy)_2]ClO_4$; (c) axial with g_z unobserved, $[TMPFe(4\text{-}HPy)_2]ClO_4$; (d) large g_{max}, $[(2,6\text{-}F_2)_4TPPFe(2\text{-}MeHIm)_2]ClO_4$; (e) large g_{max} with broad range of g values, $[(2,6\text{-}Cl_2)_4TPPFe(Py)_2]ClO_4$. The g values of these and all other complexes are reported in Table 1.

paramagnetic shifts of the pyrrole protons at low temperatures of both the $[TMPFe(L)_2]^+$ [4] and $[TPPFe(L)_2]^+$ [6,7] series of complexes and by pulsed EPR studies of related complexes, such as $[OEPFe(4\text{-}Me_2NPy)_2]^+$,[37] $[OEPFe(HIm)_2]^+$,[37] and $[TPPFe(HIm)_2]^+$[40] that confirm that the largest g value for the bis-ligand complexes with high-basicity pyridines or imidazoles is indeed aligned along normal to the plane of the heme and is thus g_z, and by single-crystal EPR spectroscopy of $[TPPFe(4\text{-}CNPy)_2]^+$ which confirms that the EPR spectrum is axial with a maximum g value of 2.62 or greater and a minimum g value of 0.92 or less.[5] Unfortunately, because of the short electron spin relaxation times and the very deep ^{14}N modulation for samples with large g_{max} EPR signals, we have thus far been unable to use the pulsed EPR techniques to confirm the orientation of the g tensor either for complexes that have a g_{max} value greater than 3.2 or less than 2.6. However, on the basis of the evidence quoted above, we are convinced that iron porphyrinate systems with g_{max} signals in which the g value is near to or less than 2.6 probably have the $(d_{xz},d_{yz})^4(d_{xy})^1$ electron configuration with an unresolved g_z value of 1.5 or considerably less. Assuming these limits to hold, the g values listed in Table 1 indicate that the lowest-basicity pyridine (4- and 3-cyanopyridine) complexes of all of the porphyrinates of this study have the $(d_{xz},d_{yz})^4(d_{xy})^1$ ground state, while the highest-basicity pyridine ($4\text{-}Me_2NPy$) complexes of all have the $(d_{xy})^2(d_{xz},d_{yz})^3$ ground state; the basicity at which each porphyrinate changes ground state appears to vary somewhat, from $pK_a(PyH^+)$ values between 2.8 and 6 for TMP and $(2,6\text{-}Br_2)_4TPP$ to <5.2 for $(2.6\text{-}F_2)_4TPP$, $\sim$5.2 for $(2,6\text{-}Cl_2)_4TPP$, and between 5.2 and 6 for $(2,6\text{-}(OMe)_2)_4TPP$, but they can only be determined by the NMR studies discussed below if the contact and pseudocontact contributions to the paramagnetic shift can be separated. Although these 4.2 K g values, or the magnetic susceptibilities along the three principal axes,[23] may vary with temper-

ature, these values may be helpful in guiding the interpretation of the NMR data obtained in this work and discussed below.

^{1}H NMR Spectra of the (2,6-X_2)$_4$TPPCo(III) Bis-pyridine and Bis-imidazole Complexes. The ^{1}H NMR spectra of the following series of cobalt complexes were recorded at ambient temperatures: [(2,6-Br_2)$_4$TPPCo(L)$_2$]BF_4 where L is 4-CNPy, 3,4-Me_2Py, and 4-Me_2NPy; [(2,6-Cl_2)$_4$-TPPCo(L)$_2$]BF_4 where L is 4-CNPy, 3-CNPy, Py, 4-MePy, 3,4-Me_2Py, 4-Me_2NPy, 1-MeIm, and 2-MeHIm; [(2,6-F_2)$_4$-TPPCo(L)$_2$]BF_4 where L is 4-CNPy, 3-CNPy, Py, 4-MePy, 3,4-Me_2Py, 4-Me_2NPy, 1-MeIm, and 2-MeHIm; and [(2,6-(OMe)$_2$)$_4$TPPCo(L)$_2$]BF_4 where L is 4-CNPy, 3,4-Me_2Py, and 4-Me_2NPy. The chemical shifts are summarized in Supporting Information Tables S4−S6. The ^{1}H NMR spectra of a series of [TMPCo(L)$_2$]BF_4 complexes listed in Supporting Information Table S7 have been reported elsewhere.[43] The chemical shifts of the proton resonances in these diamagnetic complexes are used as the diamagnetic shifts for calculating the paramagnetic shifts of the iron(III) complexes (eq 1). As can be seen, the chemical shifts follow very similar patterns from complex to complex, and thus in cases where specific complexes were not prepared, the chemical shifts can be estimated to high accuracy from the chemical shifts of related complexes.

Temperature Dependence of the ^{1}H Chemical Shifts of Low-Spin Iron(III) Porphyrinates. It should be noted that both the contact and pseudocontact terms of the paramagnetic shift have inverse temperature dependences (eq 4−7). For the pseudocontact shift, however, the temperature dependence may not be linear with inverse temperature if the second-order Zeeman term is appreciable[23] or if there are excited states of different spin multiplicities within kT of the ground state. Since the latter is found to be the case for some of the complexes of this study, some of the deviations from good linearity are probably a result of this factor.

The temperature dependence of the ^{1}H NMR shifts is best shown by a Curie plot (δ_{para} vs 1000/T), which is linear with extrapolated intercepts of zero if the Curie law is obeyed. However, curvature of the Curie plot is often observed.[8,13−15,44−46] The temperature-dependent fitting program, TDFw,[29] has been created in this laboratory and is used to fit the expanded Curie-law dependence of the chemical shift on inverse temperature in the fairly common cases of curved dependence that result from the presence of a thermally accessible excited electronic state.[12,15] The program itself can be downloaded from the Internet and used; a detailed Help section is provided.[29] In this work, we used this program to determine the energy difference, ΔE, between the ground and excited states, the spin state of the latter, and the spin densities, ρ_C, at the carbons of interest in the ground and excited states. The spin states of both the ground ($S = 1/2$ in all cases of this study) and excited states (possible $S = 1/2$, 3/2, or 5/2) are input parameters of this fitting procedure, and thus, all possible spin states for the excited state must be considered in each case. Variable-temperature ^{1}H NMR chemical shifts for all complexes are listed in the tables of Appendix A of the Ph.D. dissertation of C. T. Watson.[35] Additional variable-temperature data for three [TMPFe(L)$_2$]$^+$ complexes (L = 4-Me_2NPy, Py, 4-CNPy) were also acquired at more closely spaced temperature intervals and are essentially identical to those obtained previously;[35] the best fits were found to be to the same excited state, $S = 3/2$, and the fitted values of ΔE for the two data sets were found to be identical.

From the NMR data as a function of temperature, the program uses eq 8 to calculate the difference in energy (ΔE) between the ground and excited states for the chosen possibilities of the two. The pseudocontact contribution to the paramagnetic shift is relatively small for the pyrrole-H and *m*-H, but quite large for the *o*-H of the pyridine ligands, *o*-H_{Py}, because of the small distance ($r < 3$ Å) between the *o*-H_{Py} and the iron center (eqs 5 and 6). Thus, for the pyrrole-H and *m*-H shifts, the contact contribution dominates, and no correction has been applied for the pseudocontact contribution, while for the *o*-H_{Py} shifts the pseudocontact shift dominates, and no fits to eq 8 using the program TDFw[29] were found to converge. Because of the dissociation of axial ligands at higher temperatures, which introduces a thermodynamic equilibrium between the low-spin bis-ligand complex ground state, with its chemical shifts, and the high-spin mono-ligand complex, with its very different chemical shifts, in most cases reliable fits could only be obtained using the chemical shifts at $1000/T > 4.4$ K^{-1} or temperatures below −46 °C.

The program uses the best-fit energy difference between the ground and excited states to then calculate the Curie factors and spin densities at the carbon to which the protons of interest are bound for the ground and excited states. In cases where the pseudocontact contribution to the paramagnetic shift is very small or nonexistent, the Curie factors, C_n, are proportional to the spin densities, ρ_C, at the sites of interest and thus to their molecular orbital coefficients, which have been interpreted for the ground states of the complexes of interest to be those for the $3e(\pi)$ and $3a_{2u}(\pi)$ frontier porphyrin orbitals for the $(d_{xy})^2(d_{xz},d_{yz})^3$ and $(d_{xz},d_{yz})^4(d_{xy})^1$ ground states, respectively. However, only the 3-CNPy and 4-CNPy complexes of TMPFe(III) showed clear evidence of pure $(d_{xz},d_{yz})^4(d_{xy})^1$ ground states over the temperature range of the NMR measurements, as evidenced by a very small or even negative spin density at the β-pyrrole carbons, even though the 4.2 K EPR data for a number of other complexes indicate a pure $(d_{xz},d_{yz})^4(d_{xy})^1$ ground state. In most series of complexes, the spin densities at the β-pyrrole carbons simply decrease fairly smoothly as the pK_a(PyH$^+$) decreased, indicating that the energies of the $(d_{xz},d_{yz})^4(d_{xy})^1$ and $(d_{xy})^2(d_{xz},d_{yz})^3$ electron configurations become very similar, perhaps switch, but never separate enough to allow thermal isolation of the $(d_{xz},d_{yz})^4(d_{xy})^1$ state, even at the lowest

(44) Walker, F. A.; Nasri, H.; Turowska-Tyrk, I.; Mohanrao, K.; Watson, C. T.; Shokhirev, N. V.; Debrunner, P. G.; Scheidt, W. R. *J. Am. Chem. Soc.* **1996**, *118*, 12109−12118.
(45) Bertini, I.; Luchinat, C.; Parigi, G.; Walker, F. A. *J. Biol. Inorg. Chem.* **1999**, *4*, 515−519; 846.
(46) Simonneaux, G.; Schünemann, V.; Morice, C.; Carel, L.; Toupet, L.; Winkler, H.; Trautwein, A. X.;Walker, F. A. *J. Am. Chem. Soc.* **2000**, *122*, 4366−4377.

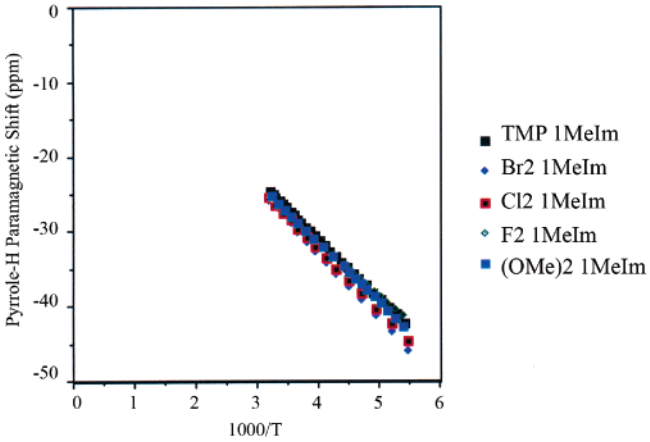

Figure 2. Plot of paramagnetic shift vs 1000/*T* for the pyrrole-H of the bis-1-methylimidazole complexes of the five iron(III) porphyrinates. Note the similar paramagnetic shifts and Curie behavior for all five complexes.

temperature used for the NMR investigations (−90 °C, 183 K). Thus, we can conclude that for all medium- to low-basicity pyridines the difference in energy between the two $S = 1/2$ ground states is considerably less than kT at 183 K or $\Delta E \leq 40$ cm^{-1}. In all cases, it was found that the paramagnetic shifts of the bis-imidazole and high-basicity pyridine complexes were best fit with the simple Curie law ($S = 1/2$, $(d_{xy})^2(d_{xz},d_{yz})^3$ ground state and no thermally accessible excited state), while most middle- to low-basicity pyridines were best fit with a two-level treatment having an $S = 1/2$ mixed $(d_{xz},d_{yz})^4(d_{xy})^1/(d_{xy})^2(d_{xz},d_{yz})^3$ electron configuration ground state and an $S = 3/2$ $(d_{xz},d_{yz})^3(d_{xy})^1(d_{z^2})^1$ electron configuration excited state with $\Delta E > 115$ cm^{-1} in all cases.

NMR Spectra of the Five Fe(III) Porphyrinates Bound to 1-Methylimidazole and 2-Methylimidazole and Their Temperature Dependences. The pyrrole-H shifts for the bis-1-MeIm complexes of the five iron(III) porphyrinates studied are all very similar, as evidenced by the Curie plots shown in Figure 2, which are all linear with intercepts near 0 ppm for all five complexes. At low temperatures, the range of pyrrole-H paramagnetic shifts is less than 5 ppm, with those of $[(2,6\text{-}Br_2)_4TPPFe(1\text{-}MeIm)_2]^+$ being the most negative, followed by $[(2,6\text{-}Cl_2)_4TPPFe(1\text{-}MeIm)_2]^+$, $[(2,6\text{-}(OMe)_2)_4TPPFe(1\text{-}MeIm)_2]^+$, then $[TMPFe(1\text{-}MeIm)_2]^+$, and finally $[(2,6\text{-}F_2)_4TPPFe(1\text{-}MeIm)_2]^+$. At +40 °C the range of paramagnetic shifts is less than 2 ppm, with the order of the paramagnetic shift values nearly the same.

For all 1-MeIm complexes, it was found that no thermally-accessible excited state existed, on the basis of the analysis of the Curie plots using the TDFw program.[29] One-level fits (simple Curie behavior) of the pyrrole-H shifts yielded very similar spin densities for all five complexes ($\rho_C = 0.0156$ (TMP), 0.0167 ($(2,6\text{-}Br_2)_4TPP$), 0.0164 ($(2,6\text{-}Cl_2)_4TPP$), 0.0156 ($(2,6\text{-}F_2)_4TPP$), and 0.0159 ($(2,6\text{-}(OMe)_2)_4$-TPP)), as summarized in Table 2.

Unlike the 1-MeIm complexes of the five iron(III) porphyrinates, the bis-2-MeHIm complexes of three of these porphyrinates have four pyrrole-H resonances at −90 °C because of the hindered axial ligand rotation, as reported previously.[47−49] For $[(2,6\text{-}Br_2)_4TPPFe(2\text{-}MeHIm)_2]^+$, four pyrrole-H resonances are observed from −90 to +20 °C, and above the latter temperature, the resonances are too broad because of the chemical exchange to accurately determine the chemical shifts. For the $[(2,6\text{-}Cl_2)_4TPPFe(2\text{-}MeHIm)_2]^+$ complex, this extreme broadening occurs above −40 °C. From −30 to +10 °C, the pyrrole-H resonances are too broad to be assigned chemical shift values. From +20 to +40 °C, however, one averaged resonance is observed. For $[TMPFe(2\text{-}MeHIm)_2]^+$, four pyrrole-H resonances are seen from −90 to −10 °C, above which the resonances are too broad for the chemical shifts to be accurately measured.[49] For $[(2,6\text{-}F_2)_4TPPFe(2\text{-}MeHIm)_2]^+$ and $[(2,6\text{-}(OMe)_2)_4TPPFe(2\text{-}MeHIm)_2]^+$, the pyrrole resonance remains a singlet throughout the −90 to +40 °C temperature range, presumably because of the smaller effective size of the fluorine and methoxy groups and thus the apparently much more rapid inversion of the porphyrin ring and ligand rotation kinetics that go along with this smaller effective size.[48]

Supporting Information Figure S1 shows the paramagnetic shift versus 1000/*T* for the pyrrole protons of the 2-MeHIm complexes of the five ferric porphyrinates. In the case where the pyrrole resonance is split into four peaks, the average value is used. The paramagnetic shifts for the ortho halogenated complexes are very similar, while $[(2,6\text{-}(OMe)_2)_4TPPFe(2\text{-}MeHIm)_2]^+$ and $[TMPFe(2\text{-}MeHIm)_2]^+$ have more positive paramagnetic shifts throughout the −90 to +40 °C temperature range. From +10 to +40 °C the pyrrole-H paramagnetic shift of $[(2,6\text{-}(OMe)_2)_4TPPFe(2\text{-}MeHIm)_2]^+$ deviates severely from the near-Curie behavior seen for the other complexes, as rapid on−off ligand exchange with increasing population of the high-spin five-coordinate intermediate shifts the resonance toward more positive chemical shift values. As found for the 1-MeIm complexes discussed above and summarized in Table 2, the temperature-dependent fitting of the pyrrole-H resonances (of all four lines for the TMP, $(2,6\text{-}Br_2)_4TPP$, and $(2,6\text{-}Cl_2)_4TPP$ complexes and the single line for the other two) led to the conclusion that there was no thermally accessible excited state, and thus spin densities were obtained from one-level (simple Curie) plots. These yielded somewhat smaller spin densities than were observed for the 1-MeIm complexes (0.0114 (TMP), 0.0145 ($(2,6\text{-}Br_2)_4TPP$), 0.0144 ($(2,6\text{-}Cl_2)_4TPP$), 0.0151 ($(2,6\text{-}F_2)_4$-TPP), and 0.0132 ($(2,6(OMe)_2)_4TPP$)).

Temperature Dependence of the ^{1}H NMR Spectra of TMPFe(III) Bound to Pyridines of Different Basicities. In comparison to the similarity in behavior of all five iron(III) porphyrinates with 1-MeIm (and to a lesser extent 2-MeHIm), the NMR spectra and temperature dependences of the ^{1}H NMR resonances of the bis-pyridine complexes ranging in basicity from 4-Me_2NPy ($pK_a(PyH^+) = 9.70$[34]) to 4-CNPy ($pK_a(PyH^+) \approx 1.1$[4]) of the five iron(III) porphy-

(47) Walker, F. A.; Simonis, U. *J. Am. Chem. Soc.* **1991**, *113*, 8652−8657; **1992**, *114*, 1929.
(48) Shokhirev, N. V.; Shokhireva, T. Kh.; Polam, J. R.; Watson, C. T.; Raffii, K.; Simonis, U.; Walker, F. A. *J. Phys. Chem. A* **1997**, *101*, 2778−2886.
(49) Momot, K. I.; Walker, F. A. *J. Phys. Chem. A* **1997**, *101*, 2787−2795.

Table 2. Summary of Results Obtained from the TDFw[29] Fits of the Temperature Dependence of δ(pyrrole-H) or δ(pyrrole-H and *m*-H_{Ph}) for the $[(2,6\text{-}X_2)_4TPPFe(L)_2]^+$ Complexes of This Study

system	GS[a]	ES[b]	ΔE[c] (cm^{-1})	MSD[d]	resonances used	β-pyrrole carbon spin densities[e] comments on quality or nature of fit
				$[TMPFe(L)_2]^+$		
L = 1-MeIm	1/2	–	–	–	pyrrole-H, *o*, *p*-CH_3, *m*-H	1: 0.0156; one-level fit
L = 2-MeHIm	1/2	–	–	–		1: 0.0114; one-level fit
L = 4-Me_2NPy	1/2	–	–	–		1: 0.0157; one-level; fair fit; only data $1000/T > 4.4$ used
L = 3,4-Me_2Py	1/2	–	–	–		1: 0.0119; one-level; fit not good
L = 3,5-Me_2Py	1/2	–	–	–		1: 0.0124; one-level; fit good
L = 4-MePy	1/2	3/2	274	0.016		1: 0.0066; OK for $S = 1/2$ d_{xy}/d_π 2: 0.0165; OK for $S = 3/2$
L = Py	1/2	3/2	338	0.004		1: 0.0055; OK for $S = 1/2$ d_{xy}/d_π 2: 0.0163; OK for $S = 3/2$
L = 3-ClPy	1/2	3/2	404	0.011		1: 0.0053; OK for $S = 1/2$ d_{xy}/d_π 2: 0.0159; OK for $S = 3/2$
L = 3-CNPy	1/2	3/2	422	0.008		1: 0.0024; OK for $S = 1/2$ d_{xy} 2: 0.0181; OK for $S = 3/2$
L = 4-CNPy	1/2	3/2	439	0.019		1: −0.0008; OK for $S = 1/2$ d_{xy} 2: 0.0193; OK for $S = 3/2$
				$[(2,6\text{-}Br_2)_4TPPFe(L)_2]^+$		
L = 1-MeIm	1/2	–	–	–	pyrrole-H, *m*-H	1: 0.0167; one-level fit
L = 2-MeHIm	1/2	–	–	–		1: 0.0145; one-level fit
L = 4-Me_2NPy	1/2	–	–	–		1: 0.0172; one-level fit
L = 3,4-Me_2Py	1/2	–	–	–		1: 0.0160; one-level fit
L = 3,5-Me_2Py	1/2	–	–	–		1: 0.0155; one-level fit
L = 4-MePy	1/2	–	–	–		1: 0.0162; one-level fit
L = 3-MePy	1/2	–	–	–		1: 0.0152; one-level fit
L = Py	1/2	3/2	130	0.032		1: 0.0082; OK for $S = 1/2$ d_π/d_{xy} 2: 0.0182; OK for $S = 3/2$
L = 3-ClPy	1/2	3/2	275	0.015		1: 0.0111; OK for $S = 1/2$ d_π/d_{xy} 2: 0.0170; OK for $S = 3/2$
L = 3-CNPy	1/2	3/2	328	0.014		1: 0.0110; OK for $S = 1/2$ d_π/d_{xy} 2: 0.0172; OK for $S = 3/2$
L = 4-CNPy	1/2	3/2	274	0.011		1: 0.0077; OK for $S = 1/2$ d_{xy}/d_π 2: 0.0185; OK for $S = 3/2$
				$[(2,6\text{-}Cl_2)_4TPPFe(L)_2]^+$		
L = 1-MeIm	1/2	–	–	–	pyrrole-H, *m*-H	1: 0.0164; one-level fit
L = 2-MeHIm	1/2	–	–	–		1: 0.0144; one-level fit
L = 4-Me_2NPy	1/2	–	–	–		1: 0.0171; one-level fit
L = 3,4-Me_2Py	1/2	–	–	–		1: 0.0163; one-level fit
L = 3,5-Me_2Py	1/2	–	–	–		1: 0.0163; one-level fit
L = 4-MePy	1/2	–	–	–		1: 0.0158; one-level fit
L= 3-MePy	1/2	–	–	–		1: 0.0153; one-level fit
L = Py	1/2	3/2	178	0.047		1: 0.0102; OK for $S = 1/2$ d_π/d_{xy} 2: 0.0173; OK for $S = 3/2$
L = 3-ClPy	1/2	3/2	449	0.011		1: 0.0132; OK for $S = 1/2$ d_π/d_{xy} 2: 0.0169; OK for $S = 3/2$
L = 3-CNPy	1/2	3/2	387	0.029		1: 0.0127; OK for $S = 1/2$ d_π/d_{xy} 2: 0.0153; OK for $S = 3/2$
L = 4-CNPy	1/2	3/2	406	0.011		1: 0.0089; OK for $S = 1/2$ d_π/d_{xy} 2: 0.0189; OK for $S = 3/2$
				$[(2,6\text{-}F_2)_4TPPFe(L)_2]^+$		
L = 1-MeIm	1/2	–	–	–	pyrrole-H, *m*-H	1: 0.0156; one-level fit
L = 2-MeHIm	1/2	–	–	–		1: 0.0151; one-level fit
L = 4-Me_2NPy	1/2	–	–	–		1: 0.0166; one-level fit
L = 3,4-Me_2Py	1/2	–	–	–		1: 0.0184; one-level; not a good fit
L = 3,5-Me_2Py	1/2	–	–	–		1: 0.0191; one-level; not a good fit
L = 4-MePy	1/2	–	–	–		1: 0.0172; one-level; good fit
L = 3-MePy	1/2	–	–	–		1: 0.0179; one-level; not a good fit
L = Py	1/2	–	–	–		1: 0.0161; one-level; good fit
L = 3-ClPy	1/2	–	–	–		1: 0.0165; one-level; not a good fit
L = 3-CNPy	1/2	1/2	287	0.022		1: 0.0171; OK for $S = 1/2$ d_π 2: 0.0019; OK for $S = 1/2$ d_{xy}
L = 4-CNPy	1/2	3/2	368	0.013		1: 0.0112; OK for $S = 1/2$ d_{xy}/d_π 2: 0.0155; OK for $S = 3/2$
				$[(2,6\text{-}(OMe)_2)_4TPPFe(L)_2]^+$		
L = 1-MeIm	1/2	–	–	–	pyrrole-H, *m*-H	1: 0.0159; one-level fit
L = 2-MeHIm	1/2	–	–	–		1: 0.0132; one-level fit
L = 4-Me_2NPy	1/2	–	–	–		1: 0.0159; one-level; not the best fit
L = 3,4-Me_2Py	1/2	–	–	–		1: 0.0164; one-level; only data below $1000/T = 4.4$ used

Table 2 (Continued)

system	GS[a]	ES[b]	ΔE[c] (cm^{-1})	MSD[d]	resonances used	β-pyrrole carbon spin densities[e] comments on quality or nature of fit
				$[(2,6\text{-}(OMe)_2)_4TPPFe(L)_2]^+$		
L = 3,5-Me_2Py	1/2	–	–	–		1: 0.0161; one-level; only data below $1000/T = 4.4$ used
L = 4-MePy	1/2	–	–	–		1: 0.0156; one-level; only data below $1000/T = 4.5$, but fit not good
L = 3-MePy	1/2	–	–	–		1: 0.0180; one-level fit
L = Py	1/2	3/2	388	0.097		1: 0.0118; OK for $S = 1/2$ d_π/d_{xy} 2: 0.0157; OK for $S = 3/2$
L = 3-ClPy	1/2	3/2	119	0.019		1: 0.0079; OK for $S = 1/2$ d_{xy}/d_π 2: 0.0127; OK for $S = 3/2$
L = 3-CNPy	1/2	3/2	409	0.011		1: 0.0043; OK for 1/2 d_{xy}/d_π 2: 0.0224; large for $S = 3/2$
L = 4-CNPy	1/2	3/2	682	0.019		1: 0.0085; OK for $S = 1/2$ d_{xy}/d_π 2: 0.0210; fit only for $1000/T > 4.5$

[a] GS = spin (S) of the ground state. [b] ES = spin (S) of the excited state. [c] Best fit energy (±30%). [d] MSD = mean-square deviation of the data points from the best fit. [e] Spin densities obtained from fits, using the program TDFw, to eq 8; 1 = ground state, 2 = excited state.

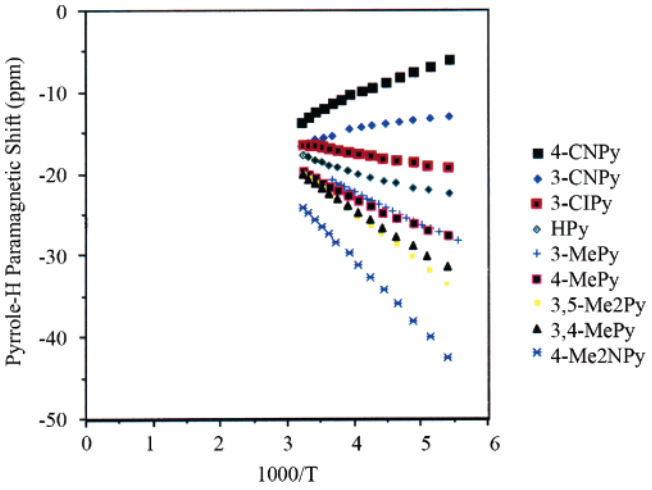

Figure 3. Plot of paramagnetic shift vs $1000/T$ for the pyrrole-H of the $[TMPFe(L)_2]^+$ complexes where L = XPy, showing the anti-Curie behavior of the low-basicity pyridine complexes and approximately Curie behavior for the high-basicity pyridine complexes.

rinates show somewhat different behaviors. The temperature dependence of the pyrrole-H, *m*-H_{Ph}, and *o*-H_{Py} are discussed in detail for the complexes of TMPFe(III), and then, comparisons in the behavior of the other four series of complexes are presented briefly. Before doing so, however, we wish to point out that the ortho substituents on the phenyl rings of all five of the iron porphyrinates of this study are large enough that phenyl rotation is not expected to occur in any of the complexes; this was shown conclusively by Eaton and Eaton for a series of (TMP)MX and five-coordinate tetra-(pentafluorrophenyl)porphyrinatometal complexes in 1975.[50] Thus, phenyl rotation is not expected to contribute in any way to the temperature dependence of the paramagnetic shifts of these complexes.

***β*-Pyrrole Protons.** Figure 3 shows the pyrrole-H paramagnetic shift vs $1000/T$ for the nine bis-pyridine complexes of TMPFe(III). For the higher-basicity pyridines, where the ligands are 4-Me_2NPy, 3,4-Me_2Py, and 3,5-Me_2Py, it can be seen that at low temperatures the pyrrole-H chemical shift is very negative and the resonances move toward the diamagnetic region linearly as the inverse temperature decreases. The curvature of the Curie plots becomes more pronounced for the middle-basicity pyridines, and for the lowest-basicity pyridine complexes, the pyrrole-H Curie plots exhibit anti-Curie behavior (Figure 3).

Table 2 summarizes the ΔE values calculated from the fits of the plots of paramagnetic shifts vs the inverse temperature for all complexes, including the series of $[TMPFe(L)_2]^+$. It was found that plots exhibiting close to true Curie behavior give a shallow minimum in the two-level fits and are best fit as one-level systems having no thermally accessible excited state. However, despite one-level fits, except for L = 1-MeIm and 4-Me_2NPy, the spin densities were smaller than the typical ρ_C at ~0.0156. For example, for L = 3,4-Me_2Py and 3,5-Me_2Py, the ρ_C values are 0.0119 and 0.0124, respectively. For L = 4-MePy, Py, 3-ClPy, and the cyanopyridines, the temperature dependence was consistent with a two-level fit with the ground state being $S = 1/2$ and the excited state being $S = 3/2$. Throughout the series of lower-basicity pyridine complexes, the values of ρ_C of the ground state decrease steadily with decreasing ligand basicity (0.0066, 0.0055, 0.0053, 0.0024, and −0.0008, respectively), indicating a ground state that has a decreasing contribution from the $(d_{xy})^2(d_{xz},d_{yz})^3$ electron configuration and an increasing contribution from the $(d_{xz},d_{yz})^4(d_{xy})^1$ electron configuration as the basicity of the ligand decreases; the 3- and 4-CNPy complexes appear to have quite pure $(d_{xz},d_{yz})^4(d_{xy})^1$ configurations. The negative value of ρ_C for the 4-CNPy complex appears to result from a small contact contribution (+) and a pseudocontact contribution of similar magnitude but opposite sign (−), as reported earlier.[15] At the same time, the values of ρ_C for the excited state generally increase somewhat (0.0165, 0.0163, 0.0159, 0.0181, 0.0193, respectively) but are still close enough to $\rho_C \approx 0.0156$ to indicate a single d_π unpaired electron for the $S = 3/2$ excited state and thus $(d_{xz},d_{yz})^3(d_{xy})^1(d_{z^2})^1$ electron configurations in all cases. From the best fits, it is found that these complexes give converged fitted ΔE values that generally *increase* with decreasing basicity of the ligand: 274 cm^{-1} for the 4-MePy complex and 439 cm^{-1} for the 4-CNPy complex.

The linear relationship between the pyrrole-H δ_{para} and the pK_a of the protonated pyridine ligands (pK_a(PyH^+)) at

(50) Eaton, S. S.; Eaton, G. R. *J. Am. Chem. Soc.* **1975**, *97*, 3660−3666.

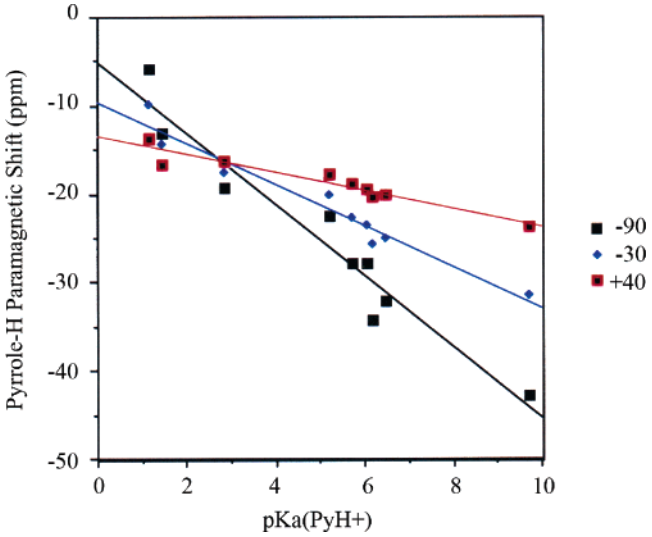

Figure 4. Plot of the paramagnetic shift of the pyrrole-H resonances of the $[TMPFe(L)_2]^+$ complexes vs $pK_a(PyH^+)$ of the axial ligands at −90, −30, and +40 °C. Note the decreasing slope of the best-fit line as the temperature increases.

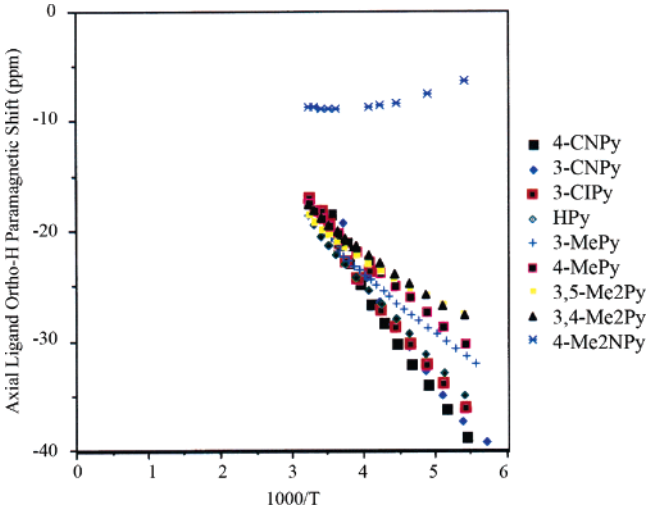

Figure 5. Plot of paramagnetic shift vs 1000/*T* for the *o*-H_{Py} of the $[TMPFe(L)_2]^+$ complexes. Note that the shifts of the low-basicity pyridine resonances are more positive than those of the higher-basicity pyridine resonances.

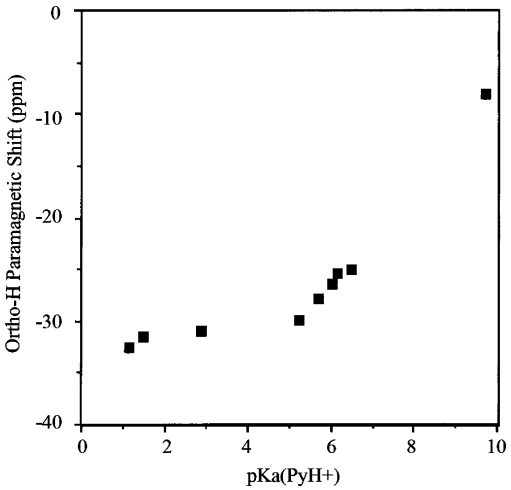

Figure 6. Plot of the paramagnetic shift of the *o*-H_{Py} at −60 °C vs pyridine basicity for the $[TMPFe(L)_2]^+$ complexes showing the slight change in slope of the line at $pK_a(PyH^+) \approx 5-6$.

−80 °C that was reported previously[4] exists throughout the temperature range studied, as shown in Figure 4. Although the slopes of these plots are negative throughout the temperature range of the measurements, they become less negative as the temperature increases.

***m*-Phenyl Protons (*m*-H_{Ph}).** The pattern of increasing paramagnetic shift with decreasing axial pyridine ligand basicity at a given temperature seen for the pyrrole-H Curie plots is also seen in the *m*-H_{Ph} Curie plots shown in Supporting Information Figure S2. The plots for each complex are linear, with only slight curvature at higher temperatures. The slope of the *m*-H Curie plot of Figure S2 for $[TMPFe(4\text{-}Me_2NPy)_2]^+$ is negative, while that of $[TMPFe(3,4\text{-}Me_2Py)_2]^+$ is close to zero, and thereafter the slopes become more positive as the axial pyridine basicity decreases further. The TDFw program[29] was not used to analyze these *m*-H_{Ph} shifts alone because of the very small temperature dependence. Rather, the *m*-H_{Ph} shifts were analyzed together with the pyrrole-H paramagnetic shifts discussed above.

Ortho Protons of the Axial Pyridine Ligands (*o*-H_{Py}). Figure 5 shows the Curie plots for the *o*-H_{Py} resonances of the TMPFe(III) complexes of the nine pyridine ligands. For the complexes with unsymmetrical pyridine axial ligands, the value plotted is the average for the two different *o*-H_{Py} resonances. For the complexes where the axial ligands are 4-CNPy through $3,4\text{-}Me_2Py$, the Curie plots show smooth shifts of the *o*-H_{Py} resonance to less negative values as the temperature is increased. A slight curvature toward more positive paramagnetic shifts can also be seen at the higher temperatures. In contrast, the *o*-H_{Py} resonance of the $[TMPFe(4\text{-}Me_2NPy)_2]^+$ complex shifts in a negative direction with increasing temperature until about 0 °C and then begins to curve in a positive direction with further-increasing temperature, likely the result of ligand dissociation. Hence, the temperature-dependent behavior of the *o*-H_{Py} resonance is entirely different from those of the pyrrole-H and *m*-H_{Ph} resonances. As will be shown in detail below, this is because the *o*-H_{Py} paramagnetic shifts have the largest pseudocontact contributions of all of the protons of these complexes, and the pseudocontact shift is sensitive to the structure and *g* anisotropy (eqs 5 and 6) rather than through-bond spin delocalization (eq 4).

A plot of the *o*-H_{Py} paramagnetic shifts at −60 °C vs $pK_a(PyH^+)$, Figure 6, as well as at all other temperatures, shows an abrupt change in slope of the best-fit line near the pK_a of the conjugate acid of pyridine itself (Py, 5.22[34]). This change in slope suggests a change in the electron configuration of the metal and thus a change in the relative contributions of the contact and pseudocontact interactions (eq 3). As the temperature is further raised, the *o*-H_{Py} resonances move somewhat further positive, but there is very little $pK_a(PyH^+)$ dependence on the *o*-H_{Py} paramagnetic shifts for the lowest-basicity pyridine complexes. Figure 5 shows that, in opposition to what is seen for the pyrrole-H shifts, the more basic pyridine *o*-H resonances deviate from Curie behavior the most, while the low-basicity pyridine complexes show fairly linear Curie behavior for the *o*-H_{Py} shifts. The *o*-H_{Py} fits to

eq 8 alone did not converge for most of the complexes for any possible excited state.

That the temperature dependences of the ligand resonances, in general, behave differently than those of the porphyrin resonances (because of ligand on−off, ligand rotation, and porphyrin inversion kinetics) has been convincingly shown for a series of bis-ligand complexes of several octaalkyltetraphenylporphyrinatoiron(III).[15] Furthermore, in the case of the iron(III) porphyrinates of this study, the strongly changing pseudocontact shift contribution, which is somewhat apparent from the g values in Table 1 and will be discussed in more detail below, begins with relatively large negative values for the most basic pyridines, where the value of $g_{\|}^2 - g_{\perp}^2$ is positive, passes through zero near the pK_a(PyH$^+$) of 4-MePy or Py, and becomes increasingly positive as the pK_a(PyH$^+$) decreases further, where the value of $g_{\|}^2 - g_{\perp}^2$ is negative, a behavior that is quite different from that expected for the contact shift, which appears to simply decrease smoothly with decreasing pK_a(PyH$^+$). This pseudocontact shift sign dependence is magnified in the case of the *o*-H_{Py} because they are very close to the paramagnetic metal center ($r < 3$ Å), and thus the use of ligand resonances to attempt to determine ΔE will not be considered further.

Temperature Dependence of the ^{1}H NMR Spectra of the [(2,6-Br$_2$)$_4$TPPFe(L)$_2$]ClO$_4$, [(2,6-Cl$_2$)$_4$TPPFe(L)$_2$]ClO$_4$, [(2,6-F$_2$)$_4$TPPFe(L)$_2$]ClO$_4$, and [(2,6-(OMe)$_2$)$_4$TPPFe(L)$_2$]ClO$_4$ Complexes where L = Pyridines of Different Basicities. Because all of these porphyrinate complexes showed similar behavior to those of the TMP complexes and to each other, their spectra are discussed together.

β-**Pyrrole Protons.** All of the complexes behave similarly, as shown in Supporting Information Figure S3 for [(2,6-Br$_2$)$_4$TPPFe(L)$_2$]ClO$_4$, Figure S4 for [(2,6-Cl$_2$)$_4$TPPFe(L)$_2$]ClO$_4$, Figure S5 for [(2,6-F$_2$)$_4$TPPFe(L)$_2$]ClO$_4$, and Figure S6 for [(2,6-(OMe)$_2$)$_4$TPPFe(L)$_2$]ClO$_4$. For all four sets of complexes, the Curie plots are linear for L = 4-Me$_2$NPy and a number of other higher-basicity pyridines, while the temperature dependences of the lower-basicity pyridine complexes show a slight curvature toward more positive paramagnetic shifts at higher temperatures, and this curvature becomes more pronounced as the basicity of the pyridine decreases. Unlike the [TMPFe(L)$_2$]$^+$ complexes, the pyrrole-H slopes are all negative except the one for the 3-CNPy complex of the dimethoxy porphyrinate, Figure S6. As Table 2 shows, the temperature dependence of the higher-basicity pyridine complexes are best fit with a simple one-level Curie plot, with the spin densities at the *β*-pyrrole positions, ρ_C, ranging from 0.0180 to 0.0152 in random order for L = 4-Me$_2$NPy to 3-MePy for the 2,6-Br$_2$, 2,6-Cl$_2$ and 2,6-(OMe)$_2$ series, while the fits of all of the [(2,6-F$_2$)$_4$TPPFe(L)$_2$]$^+$ complexes, except those having L = 3- and 4-CNPy, are best fit with a linear Curie dependence with ρ_C at the *β*-pyrrole carbons ranging from 0.0191 (3,5-Me$_2$Py) to 0.0161 (Py). The 3-CNPy complex of the 2,6-F$_2$ series was the only case in this entire study of five porphyrinates for which the two-level fit was most consistent: the ground state was found to be $S = 1/2$ $(d_{xy})^2(d_{xz},d_{yz})^3$ and the excited-state was $S = 1/2$ $(d_{xy})^1(d_{xz},d_{yz})^4$ with $\Delta E = 287$ cm^{-1}. For the 4-CNPy complex of the same 2,6-F$_2$ series, the best fit was to a mixed $S = 1/2$ ground state ($\rho_C = 0.0112$) and an $S = 3/2$ excited state ($\rho_C = 0.0155$) with $\Delta E = 368$ cm^{-1}. For Py itself and the lower-basicity pyridine complexes of the 2,6-Br$_2$, 2,6-Cl$_2$ and 2,6-(OMe)$_2$ series, the pyrrole-H shifts are best fit with a two-level plot, with reduced ρ_C for the $S = 1/2$ ground state that decreases as the basicity of the pyridine decreases and suggests a mixed d_π/d_{xy} ground state for each and a larger ρ_C for the $S = 3/2$ excited state (0.0157 to 0.0224) which suggests, in all cases, one unpaired d_π electron and a $(d_{xz},d_{yz})^3(d_{xy})^1(d_{z^2})^1$ electron configuration for all. The ΔE values range from 119 to 682 cm^{-1} among all the low-basicity pyridine complexes of the 2,6-Br$_2$, 2,6-Cl$_2$, and 2,6-(OMe)$_2$ series.

The pyrrole-H shifts for the pyridine complexes vs pK_a(PyH$^+$) at three temperatures are shown in Supporting Information Figure S7 for the 2,6-Br$_2$ series, Figure S8 for the 2,6-F$_2$ series, and Figure S9 for the 2,6-(OMe)$_2$ series of complexes: the 2,6-Cl$_2$ plot was so similar to that of the 2,6-Br$_2$ plot that it is not shown.

***m*-Phenyl Protons of the Four [2,6-(X$_2$)$_4$TPPFe(L)$_2$]$^+$ Complexes.** The *m*-H_{Ph} Curie plots of the [(2,6-Br$_2$)$_4$TPPFe(L)$_2$]$^+$ complexes shown in Supporting Information Figure S10 are similar to those of [TMPFe(L)$_2$]$^+$ except that, in this case, only the [(2,6-Br$_2$)$_4$TPPFe(4-CNPy)$_2$]$^+$ complex has a positive slope. Those of the other complexes are very similar, and for all series, the Curie plots parallel those of the respective pyrrole-H plots, as shown in Supporting Information Figures S10−S13.

Ortho Protons of the Pyridine Axial Ligands. The *o*-H_{Py} Curie plots for the [(2,6-Br$_2$)$_4$TPPFe(L)$_2$]$^+$ complexes in Supporting Information Figure S14, those for the 2,6-Cl$_2$ series in Figure S15, those for the 2,6-F$_2$ series in Figure S16, and those for the 2,6-(OMe)$_2$ series in Figure S17 show smooth shifts toward a less negative paramagnetic shift with increasing temperature for the lower basicity pyridines, as seen for the [TMPFe(L)$_2$]$^+$ complexes, although there are some differences in the order of the temperature-dependent shifts of the individual ligand complexes and an increasing overlap of the Curie plots for lower-basicity ligand complexes in the order Br = Cl < F < OMe.

In the plot of paramagnetic shift vs pK_a(PyH$^+$) at −60 °C (Supporting Information Figure S18), it is apparent that the change in slope of the best-fit line near the pK_a(PyH$^+$) found in the [TMPFe(L)$_2$]$^+$ complexes (Figure 6) is present in the [(2,6-Br$_2$)$_4$TPPFe(L)$_2$]$^+$ complexes as well but is not as pronounced as observed for the TMP complexes; the change in slope is smaller for the Cl$_2$ complexes (Supporting Information Figure S19) and is imperceptible for the F$_2$ complexes (Supporting Information Figure S20). However, for the [(2,6-(OMe)$_2$)$_4$TPPFe(L)$_2$]$^+$ series the plot of δ_{para}-(*o*-H_{Py}) vs pK_a(PyH$^+$), Figure 7, shows much less scatter in the low-basicity pyridine data than in the data for the [(2,6-F$_2$)$_4$TPPFe(L)$_2$]$^+$ complexes (Supporting Information Figure S20). Thus the change in slope of the best-fit line at pK_a(PyH$^+$) $\approx$ 5 is much more evident.

Conclusions from Temperature-Dependent Fitting of the Pyrrole-H Paramagnetic Shifts. Because of the relatively small temperature range over which ligand exchange

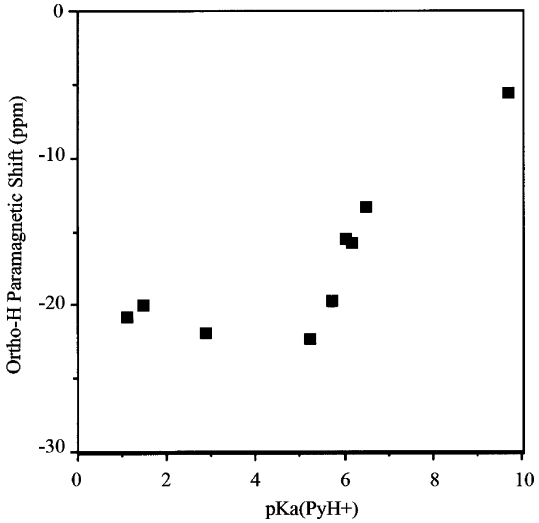

Figure 7. Plot of the paramagnetic shift of the *o*-H_{Py} at −60 °C vs pyridine basicity for the $[(2,6\text{-}(OMe)_2)_4TPPFe(L)_2]^+$ complexes, showing a definite change in slope at $pK_a(PyH^+) \approx 5$.

did not affect the chemical shifts and the relatively small number of data points obtained over that temperature range, the accuracy of the ΔE values is in general only about ±30%. Despite this, several general conclusions can be made. It is found that for the low-basicity pyridine complexes of all $(2,6\text{-}X_2)_4TPPFe(III)$ complexes the ground state is either $(d_{xz},d_{yz})^4(d_{xy})^1$ or mixed $(d_{xz},d_{yz})^4(d_{xy})^1/(d_{xy})^2(d_{xz},d_{yz})^3$ with an energy separation too small to allow us to differentiate the two states, and the thermally accessible excited state is $S = 3/2$, $(d_{xz},d_{yz})^3(d_{xy})^1(d_{z^2})^1$, with one single exception. For higher-basicity pyridine complexes, the ground state is $(d_{xy})^2(d_{xz},d_{yz})^3$ and the excited state is the same $S = 3/2$ electron configuration. For the highest-basicity pyridine and 1-MeIm, as well as 2-MeHIm complexes, the only reasonable fit was to simple Curie dependence, indicating no thermally accessible excited state. From the best fits of the Curie plots for the low-basicity pyridine complexes, it is found that these complexes give converged fitted ΔE values that generally increase as the basicity of the pyridine decreases. That the ΔE should become larger as the basicity of the pyridine decreases suggests that although the σ basicity of the pyridine toward the proton decreases, the energy of the d_{z^2} orbital of the metal appears to remain fairly constant (Scheme 1), but instead, the energy of the d_π orbitals drops so that the ΔE between lowest and highest energy of these orbitals actually increases in many (but not all) cases.

For the $[TMPFe(L)_2]^+$ complexes, the *g* values measured at 4.2 K suggest that the change in the electronic ground state occurs at or somewhat above the $pK_a(PyH^+)$ of 4-MePy (6.02) (Table 1). At the point of the change of ground state, the *g* anisotropy is zero, the d_{xz}, d_{yz}, and d_{xy} orbitals are equal in energy, and there is an equally mixed $(d_{xy})^2(d_{xz},d_{yz})^3/(d_{xz},d_{yz})^4(d_{xy})^1$ ground state. From the change in slope of the plot of the paramagnetic shift of the *o*-H_{Py} vs $pK_a(PyH^+)$ shown in Figure 5, which appears to occur between pK_a 5 and 6, we can conclude that this is the point at which the *g* anisotropy, and thus the pseudocontact shift, changes sign, and at which the two electron configurations of the ground state reverse in energy. Only in this TMP series of complexes do the two electron configurations of the ground state separate in energy from each other significantly enough that we see the spin densities at the β-pyrrole carbons that are expected for a pure $(d_{xz},d_{yz})^4(d_{xy})^1$ ground state for the lowest-basicity pyridines.

Discussion

In all of the bis-imidazole and high-basicity pyridine complexes of the five iron(III) porphyrinates under study, the electronic ground state of the metal center is low-spin d^5 $S = 1/2$ with a $(d_{xy})^2(d_{xz},d_{yz})^3$ electron configuration. The magnetic symmetry about the metal center is approximately tetragonal for porphyrin complexes that have the axial ligands lying in perpendicular planes. This is the case for all of the hindered imidazole (2-MeHIm) and substituted pyridine complexes of TMPFe(III), for which a number of structures are available,[3,4,31] and it is also expected for $(2,6\text{-}Br_2)_4TPPFe(III)$ and $(2,6\text{-}Cl_2)_4TPPFe(III)$ on the basis of the large g_{max} EPR signals observed for their bis-2-MeHIm and 4-Me_2NPy complexes (Figure 1, Table 1); by analogy, the lower-basicity pyridine complexes of these same porphyrinates are also expected to have axial ligands in perpendicular planes. However, for $(2,6\text{-}F_2)_4TPPFe(III)$ and $(2,6\text{-}(OMe)_2)_4TPPFe(III)$, while the bis-2-MeHIm complexes clearly also have axial ligands in perpendicular planes, as evidenced by the large g_{max} EPR signals, the bis-4-Me_2NPy complexes appear to have ligands in parallel planes on the basis of the rhombic EPR signals observed. Nevertheless, for the bis-4-MePy complexes of each, the EPR signal is of the large g_{max} type (Table 1), even though the steric requirements of 4-MePy binding to the iron(III) porphyrinates are not different from those of 4-Me_2NPy, and thus we cannot say with certainty whether the ligands are in parallel or perpendicular planes; in fact, these could be cases in which the dihedral angle between ligand planes is close to the 57° angle which we have recently shown to be the point at which the EPR spectral type changes from normal rhombic to large g_{max}.[51] For imidazole and the higher-basicity pyridine ligands, the unpaired electron is in an *e*-symmetry d_π (d_{xz} or d_{yz}) orbital.[3] Previous studies of low-spin iron(III) porphyrinates have shown that large negative chemical shifts at the pyrrole position arise from spin density in the *3e(π)* molecular orbital of the porphyrin ring.[6,16] These orbitals have the proper symmetry to interact with the d_{xz}, d_{yz} (d_π) metal orbitals, and the spin density can be delocalized into the *3e(π)* porphyrin orbitals through porphyrin to iron π donation. The *3e(π)* orbitals have large coefficients at four of the β-pyrrole carbons and small coefficients at the other four, with the two orbitals having large and small coefficients reversed. Because of rapid axial pyridine ligand rotation and simultaneous ruffle-inversion of the porphyrin ring,[47−49] on a time scale of millions of times per second for these metal(III) porphyrinates at ambient temperatures,[52] the spin density

(51) Yatsunyk, L. A.; Dawson, A.; Carducci, M. D.; Walker, F. A. *J. Am. Chem. Soc.* Submitted for publication, 2005.
(52) Polam, J. R.; Shokhireva, T. Kh.; Raffii, K.; Simonis, U.; Walker, F. A. *Inorg. Chim. Acta* **1997**, *263/1−2*, 109−117.

present at all eight β-pyrrole carbons is equal and is the average of the large and small spin densities of the individual *3e(π)* orbitals, on the time scale of the NMR experiments. Thus, the spin density can delocalize to the pyrrole positions and cause the large negative paramagnetic shifts seen for the pyrrole-H resonances of $[PorFe(L)_2]^+$ complexes having bis-imidazole or higher-basicity pyridine axial ligands.[6,16]

Bis-1-MeIm and -2-MeHIm Complexes of All Five Porphyrinates. For all five iron(III) porphyrinates, the temperature dependences of δ_{para} for the bis-1-MeIm complexes exhibit simple Curie behavior with no thermally accessible excited state. The β-pyrrole spin densities range from 0.0156 to 0.0167 (Table 2), a very small range of less than ±3% difference. Thus, these are the "purest" low-spin iron(III) bis-ligand complexes, which have $(d_{xy})^2(d_{xz},d_{yz})^3$ electron configurations with no contributions from other possible electron configurations. In contrast, while none of the bis-2-MeHIm complexes of the five iron porphyrinates appear to have thermally-accessible excited states, their spin densities at the β-pyrrole carbons are in general smaller (0.0151−0.0114, Table 2), suggesting an increasing contribution from the $(d_{xz},d_{yz})^4(d_{xy})^1$ electron configuration in the order of the decreasing value of ρ_C. This contribution appears to be a thermal mixing of the $(d_{xz},d_{yz})^4(d_{xy})^1$ configuration with the $(d_{xy})^2(d_{xz},d_{yz})^3$ electron configuration with a very small energy difference, ΔE. The Curie plots of the four $[TMPFe(2\text{-}MeHIm)_2]^+$ pyrrole-H resonances exhibit no evidence of the curvature that would suggest a well-separated but still thermally-accessible excited state.

The magnitude of the *g* value of the large g_{max} feature in the EPR spectra of the bis-2-MeHIm complexes of the five porphyrinates (Table 1) decreases in the same order as the value of ρ_C listed above ($g = 3.52$, $\rho_C = 0.0151$ ($(2,6\text{-}F_2)_4$TPP), 3.43, 0.0145 ($(2,6\text{-}Br_2)_4$TPP), 3.42, 0.0144 ($(2,6\text{-}Cl_2)_4$TPP), 3.35, 0.0132 ($(2,6\text{-}(OMe)_2)_4$TPP), 3.17, 0.0114 (TMP)), and previous studies of more bulky phenyl-substituted tetraphenylporphyrinates have suggested that extreme ruffling tends to push even bis-imidazole-coordinated iron porphyrinates toward the $(d_{xz},d_{yz})^4(d_{xy})^1$ electron configuration.[53,54] It is also possible that the value of g_{max} is also an indicator of the dihedral angle between the axial ligand planes, as we have recently found in X-ray crystallographic and ground crystalline EPR studies of other iron(III) porphyrinates.[51] However, there are clearly electronic as well as steric contributions to the observed electron configurations of these bis-2-MeHIm complexes. The $(2,6\text{-}F_2)_4$TPPFe(III) complex is clearly not as ruffled as the $(2,6\text{-}Br_2)_4$TPPFe(III) complex on the basis of the fact that, as mentioned above in the EPR section, the latter complex with 1-MeIm is the only one that exhibits a large g_{max} EPR spectrum at 4.2 K, indicating that the 1-MeIm ligands are in perpendicular planes.

$[TMPFe(L)_2]^+$ Complexes Where L = Substituted Pyridine. The pyrrole-H paramagnetic shifts for high-basicity pyridines (i.e., those having the $(d_{xy})^2(d_{xz},d_{yz})^3$ ground state) are dominated by the contact interaction.[6] The range of −90 °C δ_{para} values for the complexes whose Curie plots are shown in Figure 2 indicates that there are major differences in the spin density at the pyrrole position as a function of ligand basicity. The pyrrole-H δ_{para} for the 4-Me_2NPy complex at −88 °C is −42.5 ppm. For the 4-CNPy complex (the least basic pyridine studied), the pyrrole-H δ_{para} at the same temperature is −3.6 ppm. Figure 4, a plot of δ_{para} at −90, −30 and +40 °C vs $pK_a(PyH^+)$, shows that there is a smooth transition from large negative to small negative paramagnetic shift values as the basicity of the axial ligand decreases at each of these temperatures.

For low-basicity pyridine complexes of TMPFe(III), such as $[TMPFe(4\text{-}CNPy)_2]^+$, it is found, from the EPR spectra,[4,5] that the d_{xy} orbital is of higher energy than the degenerate (d_{xz},d_{yz}) set and contains the unpaired electron.[5,44] The d_{xy} orbital, however, does not have the proper symmetry to overlap with any porphyrin orbital unless the TMPFe(III) bis-pyridine complexes are S_4 ruffled.[5] In this case, the lobes of the d_{xy} orbital, which are in the mean plane of the porphyrin ring, have the correct symmetry for partial overlap with the nitrogens of the the $3a_{2u}(\pi)$ porphyrin orbital because a component of each of the nitrogen p_z orbitals lies in the *xy* plane of the porphyrin ring. This allows porphyrin-to-metal π electron donation, and spin density can thus be delocalized to the $3a_{2u}(\pi)$ molecular orbital. This porphyrin molecular orbital has small electron density at the β-pyrrole positions and large orbital coefficients at the meso carbons.[6] This results in small shifts for pyrrole-H resonances from their diamagnetic positions for the $[TMPFe(L)_2]^+$ complexes with lower-basicity pyridine axial ligands and large negative shifts of the *m*-H resonances of $[OEPFe(t\text{-}BuNC)_2]^+$ or large negative shift differences of porphyrin phenyl-H and ($\delta_m - \delta_p$) or ($\delta_m - \delta_o$) of $[TPPFe(t\text{-}BuNC)_2]^+$.[18] The orbital overlap is made possible by the S_4 ruffling of the porphyrin core found in these complexes.[5,18,44]

The Curie plots of the pyrrole-H resonances of the series of pyridine complexes of TMPFe(III) (Figure 3) show clearly that there is a range of behaviors, from Curie to anti-Curie, as the basicity of the pyridine decreases. The inverse temperature dependence seen in eq 4 for the contact and eqs 5 and 6 for the pseudocontact components of the paramagnetic shift suggests that there should be a smooth linear shift of the pyrrole-H resonance toward zero paramagnetic shift as the temperature is raised. This can clearly be seen for both the 4-Me_2NPy and 3,5-Me_2Py complexes of TMPFe(III), where the Curie plots for these two ligand complexes, shown in Figure 8, are linear and extrapolate to near 0 ppm at $1/T = 0$. The lowest-basicity pyridine complex pyrrole-H resonances show anti-Curie behavior, with curved lines and very negative apparent intercepts for the lowest-temperature part of the plots. This difference from the expected Curie behavior can be explained by two possible effects: (1) the presence of a thermally-accessible excited state and (2) the rapid ligand on−off exchange with a five-coordinate intermediate of increasingly significant concentration as the temperature is raised. Each of these processes results in a

(53) Nakamura, M.; Tajima, K.; Tada, K.; Ishizu, K.; Nakamura, N. *Inorg. Chim. Acta* **1994**, *224*, 113−124.
(54) Nakamura, M.; Ikeue, T.; Fujii, H.; Yoshimura, T.; Tajima, K. *Inorg. Chem.* **1998**, *37*, 2405−2414.

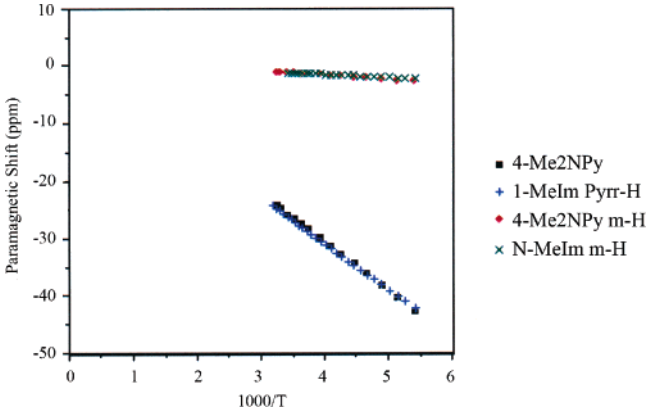

Figure 8. Curie plot showing the similar temperature dependence of the pyrrole-H and *m*-H_{Ph} of $[TMPFe(1\text{-}MeIm)_2]^+$ and $[TMPFe(4\text{-}Me_2NPy)_2]^+$.

different electronic state for the complex as the temperature is raised and thus different paramagnetic shifts for the pyrrole protons.

The presence of a thermally accessible electronic excited state has been discussed in the Results section, where fitting of the paramagnetic shifts to eq 8 was used to estimate the energy separation between ground and excited states and the nature of the latter, as well as the spin density coefficients for the β-pyrrole carbons for both the ground and excited states. It has been shown previously by EPR and Mössbauer spectroscopies,[4,10] as well as MCD spectroscopy,[10,42] all recorded at 4.2 K, that the ground-state electronic configuration of $[TMPFe(4\text{-}CNPy)_2]^+$ has the unpaired electron in the d_{xy} orbital, while the excited state, found by temperature-dependent fitting of the paramagnetic shifts in this work, has $S = 3/2$, with β-pyrrole spin densities, ρ_C, that are similar to or slightly larger than those of the $S = 1/2$ $(d_{xy})^2(d_{xz},d_{yz})^3$ ground-state complexes ($\rho_C = 0.0159-0.0193$). As mentioned in the Results section, this similarity suggests that the electron configuration of the $S = 3/2$ excited state is $(d_{xz},d_{yz})^3(d_{xy})^1(d_{z^2})^1$ rather than $(d_{xy})^2(d_{xz},d_{yz})^2(d_{z^2})^1$, where the spin densities at the β-pyrrole carbons should be approximately double these quantities because of the presence of two d_π unpaired electrons. Thus, the unpaired electron in the d_π orbital has the proper symmetry to overlap with one of the $3e(\pi)$ molecular orbitals of the porphyrin, resulting in spin delocalization to the pyrrole positions of a magnitude similar to that observed for the $S = 1/2$ $(d_{xy})^2(d_{xz},d_{yz})^3$ ground-state complexes. This causes the resonance to shift toward less positive paramagnetic shifts as the temperature is increased. This explains the anti-Curie behavior seen in the 4-CNPy and 3-CNPy complexes of TMPFe(III), as well as the trend seen as the slopes of the lines move smoothly from negative to positive as the basicity of the ligand decreases through the series 4-MePy to 4-CNPy. By the time the 3-CNPy and 4-CNPy complexes are reached, the ground state has switched to a quite pure $S = 1/2$ $(d_{xz}, d_{yz})^4(d_{xy})^1$ electron configuration with the excited state continuing to be the $S = 3/2$ $(d_{xz},d_{yz})^3(d_{xy})^1(d_{z^2})^1$ electron configuration. An increase in the population of this excited state thus shifts the pyrrole-H resonance in a negative direction as the temperature increases. Scheidt et al.[55] found that a related six-coordinate complex, $[OEPFe(3\text{-}ClPy)_2]^+$, has an intermediate-spin iron center, and the bis-4-Me_2NPy and 4-CNPy complexes of OETPPFe(III), OMTPPFe(III) and $TC_6TPPFe(III)$[15] show $S = 3/2$ excited states. It is thus not surprising that $S = 3/2$ excited states are observed for the complexes in the present study.

The other process that causes nonlinear behavior in the Curie plots is ligand dissociation because of the decreasing size of the equilibrium constants for bis-ligand complex formation as the temperature is raised, combined with rapid on−off ligand exchange between the bis- and mono-ligand complexes, which averages the chemical shifts for the five- and six-coordinate complexes. The ^{1}H NMR spectra for many of these complexes, especially the lower-basicity pyridine complexes, show broadening of the pyrrole-H, *o*-H_{Py}, and free ligand resonances as the temperature is raised above −30 °C, a clear sign of a kinetic process involving an intermediate with a different spin state. For strong donors, such as the more basic pyridine ligands of this study, the five-coordinate mono-ligand complex is expected to be high-spin, $S = 5/2$, as seen in the five-coordinate TMPFeCl complex. In the chloroiron(III) high-spin species, the pyrrole-H resonance lies at +81 ppm at room temperature (Table S2), and a mono-pyridine complex would be expected to have a similar pyrrole-H chemical shift. As the temperature is raised to the point where chemical exchange of the six-coordinate low-spin complex with the five-coordinate high-spin complex becomes apparent by broadening of the free and bound ligand resonances, the position of the pyrrole-H resonance of the (ostensibly) low-spin complex shifts in a positive direction more rapidly than expected and the temperature dependence plot thus curves toward more positive chemical shifts than expected for Curie behavior.

For the lower-basicity pyridines, however, the five-coordinate complex could have the intermediate-spin $S = 3/2$ state (and of course, a spin-admixed state would also be possible). This $S = 3/2$ state is seen in the five-coordinate $TMPFeOClO_3$ complex, with $OClO_3^-$ being a fairly weak-field axial ligand. (The ^{1}H NMR spectra of the porphinatoiron(III) perchlorate complexes used in this study are summarized in Supporting Information Table S3.) With the low-basicity pyridines also being fairly weak-field ligands, it would not be surprising if their five-coordinate TMPFe(III) complexes were also intermediate-spin or spin-admixed. Because the $d_{x^2-y^2}$ orbital is not populated for the $S = 3/2$ (or is only partially populated for spin-admixed) iron porphyrinates, the five-coordinate mono-pyridine complexes have similar or more negative pyrrole-H shifts than those of the $S = 1/2$ $(d_{xy})^2(d_{xz},d_{yz})^3$ ground-state complexes, depending upon the electron configuration of the $S = 3/2$ or spin-admixed $S = 3/2$, 5/2 five-coordinate complex, although this does depend on the 2,6-phenyl substituents,[13] as shown in Table S3. Thus, the ligand on−off exchange with an intermediate with a different spin state is a major factor which must be considered in interpreting the temperature-dependence data for the lower-basicity pyridines; at temperatures

(55) Scheidt, W. R.; Geiger, D. D.; Hayes, R. G.; Lang, G. *J. Am. Chem. Soc.* **1983**, *105*, 2625−32.

above −46 °C (1000/T = 4.4), in this study, it is evident that ligand dissociation plays a role in determining the observed chemical shifts of all porphyrin resonances, while for the higher-basicity pyridines, this does not appear to be the case. The latter ligands bind to TMPFe(III) with larger equilibrium constants,[56] and evidence of chemical exchange, such as line broadening in the NMR spectra, is not observed until the temperature is raised to +30 to +40 °C. Nevertheless, the temperature-dependent fitting of the Curie plots used data recorded at below −45 °C in all cases.

To investigate the pseudocontact contribution to the paramagnetic shift, we examined the *o*-H resonances of the axial pyridine ligands in detail. The pseudocontact shift exhibits r^{-3} dependence (eq 6), and thus the protons closest to the iron center have the largest pseudocontact shifts; *o*-H_{Py} are only on average 2.98 Å from the Fe center.[3,4] To determine if there is a trend in the shifts of the *o*-H_{Py} resonances of the different complexes, we constructed plots of the *o*-H_{Py} paramagnetic shift vs pK_a(PyH^+) at −60 °C for each of the iron(III) porphyrinate series (Figures 6, 7, S18−S20). From these plots it is evident that in each case there is a change in the slope of the line at roughly the pK_a of the conjugate acid of pyridine itself, with steeper slope for the higher-basicity pyridines and a less steep slope for the lower-basicity pyridines.

The 4.2 K EPR data for the $[TMPFe(L)_2]^+$ complexes with pyridine axial ligands (Table 1), together with NMR,[4,7] MCD,[42] and pulsed EPR data,[37,40] show that the sign of the magnetic anisotropy changes throughout the series of ligands. Thus, for basic pyridine complexes, such as $[TMPFe(4\text{-}Me_2NPy)_2]^+$, $g_z > g_x, g_y$, indicating that the unpaired electron is in the d_{xz},d_{yz} orbital set, while for the weakly basic pyridine complexes, such as $[TMPFe(4\text{-}CNPy)_2]^+$, $g_x, g_y > g_z$, indicating that the unpaired electron is in the d_{xy} orbital. A change in sign of the magnetic anisotropy will change the sign of the pseudocontact shift (eq 6). The *o*-H_{Py} resonances are the most sensitive to changes in the pseudocontact shift, and because there is a pronounced change in slope of the *o*-H_{Py} paramagnetic shift vs pK_a(PyH^+), it can be reasoned that this change in the sign of the magnetic anisotropy occurs between a pK_a of 5 and 6 for the TMP complexes. It should be noted, however, that the ligand basicity at which the thermally accessible S = 3/2 excited state begins to be detected is similar, and thus, the changes in the electron configuration and thermal excitation appear to occur hand-in-hand. This has less influence on our understanding of the TMPFe(III) complexes than of the other four iron porphyrinates, as will become evident below.

Separation of the Contact and Pseudocontact Shifts for $[TMPFe(L)_2]ClO_4$. The ability to separate the contact and pseudocontact shifts of a series of related metalloporphyrinate complexes is an obvious sign that the magnetic properties of the systems of interest are clearly understood. In the present study, the TMP complexes are the only ones that permit this separation with any degree of confidence, even though the gross magnetic behavior of all five sets of porphyrinate complexes appears to be fairly similar. The separation method and results are discussed in detail in the Supporting Information. As a summary, we can say that the plot of paramagnetic shift of the *o*-H_{Py} resonance vs pK_a(PyH^+) (Figure 6) and the paramagnetic shift of the *m*-H_{Ph} resonance of the bis-(4-Me_2NPy) complex of TMPFe(III) (which was assumed to be totally pseudocontact in nature)[6,16,24] play central roles in separating the contact and pseudocontact shifts.

With the assumption that the *m*-H_{Ph} paramagnetic shift is totally pseudocontact in nature, the pseudocontact shift of the *o*-H_{Py} of $[TMPFe(4\text{-}Me_2NPy)_2]^+$ could be calculated from the ratio of the geometric factors for the *m*-H_{Ph} and *o*-H_{Py} protons for the TMPFe(III) complex (Supporting Information Table S8). From that value of δ_{pc} of the *o*-H_{Py}, δ_{con} for these protons could immediately be calculated from δ_{para} for the same protons (eq 3). Now, with the assumption that δ_{pc} becomes zero at a ligand basicity close to that of Py or 4-MePy, the δ_{para} of the *o*-H_{Py} for that complex is identically equal to δ_{con}. Using these two contact shift data points, a straight line representing the dependence of δ_{con} on pyridine basicity can be drawn in Figure 6 to produce a new version of it (Supporting Information Figure S21) which allows δ_{con} and δ_{pc} of the *o*-H_{Py} of each complex to be determined. Then, using the geometric factors for the *o*-H_{Py}, *m*-H_{Ph}, and pyrrole-H from Supporting Information Table S8, the values of δ_{pc} for the *o*-H_{Py} can be used to calculate those for the *m*-H_{Ph} and pyrrole-H of each complex.

Thus, the change in the slope of the plot of δ_{para}(*o*-H_{Py}) at a pK_a(PyH^+) close to that of Py or 4-MePy (Figure 6) *is indicative of a change in sign of the g anisotropy*, eq 6, and hence *a change in the relative energy ordering of the d_{xy} and d_π orbitals of the metal*. The results, presented in Supporting Information Table S9 for the nine TMPFe(III) complexes using 4-MePy as the point at which the *g* anisotropy changes sign, show that the pyrrole-H contact shift at −60 °C decreases in magnitude from −27.7 ppm for L = 4-Me_2NPy to −14.6 ppm for L = 4-CNPy, while the pseudocontact shift of the same protons varies from −8.6 to +6.4 ppm over the same series.

$[(2,6\text{-}Br_2)_4TPPFe(L)_2]ClO_4$, $[(2,6\text{-}Cl_2)_4TPPFe(L)_2]ClO_4$, $[(2,6\text{-}F_2)_4TPPFe(L)_2]ClO_4$, and $[(2,6\text{-}(OMe)_2)_4TPPFe(L)_2]ClO_4$ Complexes. For all of these complexes, it can be seen from the spin densities at the β-pyrrole carbons (Table 2) that all low-basicity pyridines have mixed S = 1/2 $(d_{xy})^2(d_{xz},d_{yz})^3/(d_{xz},d_{yz})^4(d_{xy})^1$ ground states over the temperature range of the NMR measurements *plus* a thermally-accessible S = 3/2 excited state that contributes signficantly to the NMR paramagnetic shifts, even at −60 °C (213 K). Thus, none of the low-basicity pyridine complexes of these four iron(III) porphyrinates has a pure $(d_{xz},d_{yz})^4(d_{xy})^1$ ground state over the temperature of the NMR measurements. The EPR spectra, however, show that at 4.2 K the complexes from L = 4-HPy to 4-CNPy all have the $(d_{xz},d_{yz})^4(d_{xy})^1$ ground state.

For all of the $[(2,6\text{-}X_2)_4TPPFe(L)_2]^+$ complexes, the *o*-H_{Py} δ_{para} vs pK_a(PyH^+) plot was examined to obtain evidence for the basicity at which the *g* anisotropy changes sign. And

(56) Nesset, M. J. M. The Effect of Axial Ligands and Porphyrin Substituents on the Dynamic and Electronic Properties of Model Hemes. Ph.D. Dissertation, University of Arizona, Tuscon, AZ 1994.

in all cases, there is a change in slope of the pK_a(PyH^+) near the parent Py data point (5.22). If the pseudocontact shift is zero at this point and the $[(2,6\text{-}X_2)_4TPPFe(4\text{-}Me_2\text{-}NPy)_2]^+$ complex of each has the purest $(d_{xy})^2(d_{xz},d_{yz})^3$ ground state, the *o*-H_{Py} contact shift for $[(2,6\text{-}X_2)_4TPPFe(4\text{-}Me_2\text{-}NPy)_2]^+$ at −60 °C can be calculated and a similar determination of the pseudocontact and contact shifts of the lower-basicity pyridines to that discussed above for the TMPFe(III) complexes could be carried out. However, such treatments show increasingly (rather than decreasingly) negative contact shifts for the pyrrole-H resonance as the basicity of the pyridine is decreased, which are inconsistent with the expectation that the contact shift should become less negative as the transition to the $(d_{xz},d_{yz})^4(d_{xy})^1$ ground-state becomes more complete, as found for the $[TMPFe(L)_2]^+$ complexes discussed above. Other assumptions, including using the spin density determined for the pyrrole β-carbons of the bis-4-CNPy complexes of each iron porphyrinate (Table 2) to estimate the degree of transition from the $(d_{xy})^2(d_{xz},d_{yz})^3$ to the $(d_{xz},d_{yz})^4(d_{xy})^1$ ground state throughout the series of pyridine complexes for each at best gave a fairly constant contact shift throughout the series. Thus, it is clear that the mixed-orbital ground state of most lower-basicity pyridine complexes and the presence of a thermally accessible $S = 3/2$ excited state in each case preclude the separation of the pseudocontact and contact contributions to the paramagnetic shifts of the ground states of the four $[(2,6\text{-}X_2)_4TPPFe(L)_2]^+$ series of iron(III) porphyrinates, and the changes in slope of the *o*-H_{Py} paramagnetic shift vs pK_a(PyH^+) observed for these four series of iron(III) porphyrinates are likely to be the result of the increasing contribution from the $S = 3/2$ excited state as the ligand basicity is decreased.

Conclusions. The ^1H NMR spectra of the $[TMPFe(L)_2]^+$ and $[(2,6\text{-}X_2)_4TPPFe(L)_2]^+$ complexes as a function of temperature exhibit a range of behaviors. The $[TMPFe(L)_2]^+$ paramagnetic shifts encompass every situation seen in the other complexes, from the purest $(d_{xy})^2(d_{xz},d_{yz})^3$ ground state of the $[TMPFe(4\text{-}NMe_2Py)_2]^+$ complex, which demonstrates Curie behavior, to the $[TMPFe(4\text{-}CNPy)_2]^+$ complex which shows definite anti-Curie behavior resulting from a quite pure $(d_{xz},d_{yz})^4(d_{xy})^1$ ground state with thermal population of the $S = 3/2$ $(d_{xz},d_{yz})^3(d_{xy})^1(d_{z^2})^1$ excited state. For $[(2,6\text{-}Br_2)_4TPPFe(L)_2]^+$, $[(2,6\text{-}Cl_2)_4TPPFe(L)_2]^+$, $[(2,6\text{-}F_2)_4TPPFe(L)_2]^+$, and $[(2,6\text{-}(OMe)_2)_4TPPFe(L)_2]^+$, the complexes with higher-basicity pyridine axial ligands also show Curie behavior, while the low-basicity complexes show non-Curie behavior. None show the anti-Curie behavior seen for $[TMPFe(4\text{-}CNPy)_2]^+$ and $[TMPFe(3\text{-}CNPy)_2]^+$ (Figure 3).

When one attempts to separate the contact from the pseudocontact shifts using the δ_{para}(*o*-H_{Py}) vs pK_a(PyH^+) plots, it becomes apparent that the contact shift line calculated by assuming the *m*-H_{Ph} shift of $[TMPFe(4Me_2NPy)_2]^+$ is totally pseudocontact in nature and then using the geometric factors of the *m*-H_{Ph} and the 4-NePy $\delta_{para} = \delta_{con}$ point of the *o*-H_{Py} vs pK_a(PyH^+) plot of Figure S21 leads to the best estimate of the contact shifts. However, the same procedure does not work for the other four series of Fe(III) porphyrinates.

Acknowledgment. The financial support of the National Institutes of Health (Grant DK-31038) is gratefully acknowledged. The authors wish to thank Professor Michael F. Brown of the University of Arizona and Professor Ursula Simonis of San Francisco State University for use of NMR spectrometers for part of this work. This paper was written while F.A.W. was an Alexander von Humboldt Awardee in Science in the Physics Institute at the University of Lübeck. She wishes to thank her host, Professor Alfred X. Trautwein, for his hospitality and friendship during this stay.

Supporting Information Available: Figures S1−S20 and Tables S1−S7. This material is available free of charge via the Internet at http://pubs.acs.org.

IC0507316